Improvement of Long-Term Performance of Unpaved Road Constructed over Marginalized Subsoil using Geotextile Reinforcement

Nayan Jyoti Sarma, Arindam Dey

Nayan Jyoti Sarma
Research Scholar, Department of Civil Engineering, Indian Institute of Technology Guwahati, India. Email: nayan.jyoti@iitg.ac.in

Arindam Dey*
Associate Professor, Department of Civil Engineering, Indian Institute of Technology Guwahati, Assam, India. Contact No.: +918011002709, ORCID ID: 0000-0001-7007-2729
Email: arindam.dey@iitg.ac.in

* Corresponding author

Funding:
This research did not receive any specific grant from funding agencies like public, commercial or non-profit sectors.

Declarations of Interest
None

Improvement of Long-Term Performance of Unpaved Road constructed over marginalized Subsoil using Geotextile Reinforcement

ABSTRACT

Conventional design of unpaved road is based on a two-dimensional plane strain approach with no residual deformation along the length of the road. However, in reality, the nature of vehicular load distribution is three dimensional. In this study, firstly, by considering the shape and dimension of equivalent wheel contact, analytical formulations are developed based on a limit equilibrium approach to determine the thickness of unpaved road resting on a generalized marginal subgrade. Further, to overcome the basic assumption of limit equilibrium approach that considers the unpaved road system to be rigid while neglecting any deformations, a Finite Element based study is conducted to incorporate the influence of deformations in improving the design of unpaved road. Based on a coupled stress-deformation approach, a step-by-step design methodology of unreinforced unpaved road is developed by duly incorporating the operational failure conditions under quasi-static loading condition. In order to avert the operational failures, application of geotextile layer at the aggregate-subgrade interface is found to successfully reduce the stresses transferred to the subgrade, thereby exhibiting its benefit in enhancing the long-term performance of unpaved roads. Furthermore, the influence of quasi-dynamic repetitive loading condition for different numbers of vehicle passes is also exhibited for both unreinforced and reinforced unpaved roads. It is observed that with increase of vehicle passes, substantial rutting is exhibited in the unreinforced condition that surpasses the serviceability criteria beyond certain cycles of loading. Inclusion of geotextile layer at the aggregate-subgrade interface is found to successfully counteract the surface rutting and vertical displacements. Through the FE-based analysis reported in the present study, the sustainable application of geotextile in unpaved road design and enhancing its long-term performance under repetitive loading is successfully highlighted.

Keywords: Geotextile-reinforced unpaved roads, Finite element-based design, Operational conditions, Aggregate thickness, Rutting, Sustainable application

1. Introduction

According to the global studies, unpaved road comprises about 80-85% of the world's road network [1]. In developing countries like India [2] and even in developed countries such as USA [3, 4], 35%-65% of the road network is still unpaved. The most common type of unpaved roads is the gravel road or non-paved surface roads. A typical gravel road consists of an aggregate layer directly placed over the natural soil subgrade [5, 6] without immediate application of any binder material such as asphalt or cement [7]. In general, unpaved roads carry low volume of traffic; thus, it is often economically viable to surface them with a bituminous seal if the average annual daily traffic (AADT) increases more than 300 [8]. However, in some cases, unpaved roads also need to carry heavier vehicles such as in case of the access road to industrial plants, mining sites, construction sites, and connecting or supply roads of goods from major village to nearby highways [8]. In specific scenarios, owing to the unavailability of good quality material or for some site-specific restrictions, engineers are compelled to construct the unpaved roads on weak or marginalized soils having low bearing resistance. In such cases, unpaved road undergoes short-term or long-term deformation such as rutting, corrugation, potholes, washboard formations and surface degradations leading to dust emissions [9-12]. In such cases, regular maintenance work such as

replacing the unpaved road material (aggregate, soil subgrade) or incorporating soil stabilization technique (dynamic compaction, mixing of admixtures etc.) becomes significant for prolonging the durability of the unpaved road. However, regular maintenance work at regular intervals each time becomes highly cost incurring due to the involvement of man power and natural raw material extraction. Ground improvement techniques for subgrade strengthening induce more longevity to the unreinforced unpaved roads; yet such methods are significantly cost incurring processes and resource equipment demanding. In this regard, use of geosynthetic as reinforcement in unpaved road structure has emerged as a sustainable and economical solution to the problem [13, 14]. In comparison to ground improvement techniques, laying of geotextiles at the aggregate-subgrade interface is a comparatively less time-consuming and less equipment-intensive process. Moreover, the performance life of the geotextiles is significantly high, which results in substantially lesser long-term maintenance costs. Hence, from the view of economic viability, application of geotextiles to construct reinforced unpaved roads has more long-term economic feasibility. However, to get a realistic assessment, a cost-benefit analysis needs to be done, which is beyond the purview of the present study.

The applications of geosynthetics in areas such as civil, geotechnical, transportation, environmental etc. includes filtration, drainage, protection, separation, slope stabilization, soil reinforcement and stabilization [15, 16]. There are various types of geosynthetics available commercially in planar or three-dimensional form such as geotextile, geogrids, geomembranes, geocomposites and geocells [17]. Out of all geosynthetics, geotextiles and geogrids are extensively used in unpaved roads [7, 18, 19]. Generally, geosynthetic reinforcements are placed at the aggregate and subgrade interface to improve the performance of unpaved road [20, 21]. Due to the tension membrane effect in geotextile [22] and the interlocking effects imparted by geogrids [7], the lateral movement of the aggregate materials is restrained, thereby improving the load distribution to the subgrade layer and consequently increasing the bearing capacity of the subgrade layer [14]. Over the decades, researchers have conducted experimental and numerical studies on the application of geosynthetics in unpaved road. Giroud and Noiray [22] conducted pioneering quasi-static analyses for the design of unpaved roads resting on a saturated cohesive subgrade with low permeability. The beneficial effect of placing a single layer geotextile reinforcement at the aggregate-subgrade interface was exhibited by lowered rut depths and capacity to carry higher number of vehicular passes. It was also observed that due to the geotextile reinforcement, the aggregate thickness required to sustain the vehicular axle load can be reduced. Holtz and Sivagukan [23] extended the pioneering work for different rut depths (defined as the additive of the maximum settlement occurring beneath the wheels and the maximum heaving occurring in between the wheels). It was found that for smaller rut depths, the geotextile primary worked as separator; however, at larger rut depths, the geotextile behaved as reinforcement. Bourdeau *et al.* [24] conducted an analytical study to critically examine the large-scale strip loading test of geotextile-reinforced unpaved roads on peat performed by Douglas and Kelly [25]. Through this study, the influence of geotextile anchorage and stiffness modulus on the soil-geotextile interaction and interface response was examined. The results from loading test suggested that there is no significant difference in the performance of unpaved roads with a woven or a non-woven geotextile or even a polyethylene film separator with different anchorage conditions and tensile moduli. Following the work by Giroud and Noiray [22], Milligan *et al.* [26, 27] presented a new method for the design of unreinforced and reinforced unpaved roads under plane strain condition by considering the development of shear stresses at the subgrade-fill interface. The analysis demonstrated the efficiency of reinforcement under both

smaller and larger rut depths. Tingle and Webster [28] conducted a full-scale test to validate the design criteria proposed by Army and Air Force [29] for geotextile reinforced unpaved roads and modified the same for including a stiff biaxial geogrid reinforcement. From the tests conducted by Tingle and Webster [28], comprising a moving load generated by 2000 passes of military trucks having single front axle weight of 4.76 tons and dual-tandem rear axle of weight 15 tons, it was observed that the bearing capacity factor for geotextile-reinforced unpaved road is unconservative as compared to the theoretical results [28]. Giroud and Han [30, 31] developed a generalized methodology to estimate the required thickness of the base course (aggregate layer) in reinforced unpaved roads with a single layer of geogrid placed at the aggregate-subgrade interface. Tingle and Jersey [32] conducted laboratory cyclic plate load tests on six instrumented model test pavements. The results indicated that for the same aggregate layer thickness, reinforced pavement sections exhibited an improvement in the resistance to rutting. However, at the same time, it was also noted that unreinforced sections with an additional 150 mm base thickness exhibited better performance than the corresponding reinforced section. Hufenus *et al*. [33] conducted full scale field test on the application of variation in geogrid stiffness on the reduction in rut depth formation of the unpaved road structure. Lyons and Fannin [34] highlighted the importance of proper choice and consistency of parameters while dealing with the semi-empirical design of unpaved roads.

Research on unpaved roads experienced a substantial rejuvenation from the last decade. From a comparative study by Latha *et al*. [35], excessive rutting was observed for unreinforced section after 17 passes, however reinforced sections were operational beyond 250 vehicle passes except for a single geotextile reinforced unpaved road section that failed at 100 passes. Mekkawy *et al*. [36] conducted a field and laboratory study to investigate the application of biaxial geogrids on the rutting of a 310 m stretch granular shoulder overlying a clayey subgrade layer (California bearing ratio, CBR<10) subjected to repeated traffic loads. A year-long monitoring indicated that the shoulder rutting is eliminated along with a perceptive increase in CBR value. Perkins *et al*. [37] applied the mechanistic-empirical modeling methods previously developed for geosynthetic base-reinforced flexible pavements to reinforced unpaved roads. The model provides necessary information of rutting formation in unpaved road and the importance of excess pore pressure assessment on the stability of the structure. Yang *et al*. [38] conducted accelerated pavement testing (APT) to evaluate the performances of a novel polymeric alloy (NPA) geocell in improving the stability of unpaved road sections with sand bases under wheel load. The strain gauge measurements exhibited the development of tensile stresses in the NPA geocell beneath the wheel path, while compressive stresses were noted in the geocells outside the wheel path. Ravi *et al*. [39] conducted a series of model-scaled tests to understand the performance of reinforced unpaved road systems constructed on clayey subgrade of various strengths under repetitive loading. The results indicated that the efficacy of the reinforcement in reducing the settlement reduces with the strength of the subgrade layer and its usage becomes irrelevant beyond an undrained shear strength (s_u) of 30 kPa. Wu *et al*. [40] conducted loaded wheel tester (LWT) to evaluate the reinforcing effect of four different geogrids reinforcement with different apertures and stiffness in three unbounded granular base materials under repeated loading. The LWT test results successfully exhibited the beneficial effects of using geogrid reinforcement in the base course in improving the rutting resistance as indicated by the improved values of traffic benefit ratio (TBR) and rutting reduction ratio (RRR). With the aid of laboratory-based repeated plate load test, Nair and Latha [20] succinctly presented the effect of type, quantity, position and form of geosynthetic reinforcement on the measured deformations and surface profiles of unpaved road sections

constructed on clayey subgrade. The results successfully illustrated benefit of using geosynthetics is introducing higher magnitudes of elastic or recoverable settlement and arresting the plastic settlement. From similar tests, Suku *et al*. [41] elucidated that application of geocell reinforcement in base courses of unbounded roads can reduce the permanent deformation by almost 70% as compared to the unreinforced sections. Apart from arresting rutting, the application of geosynthetic reinforcement is also aids in reduction in the thickness of aggregate layer as much as 50% as compared to unreinforced section, thereby paving the pathway of achieving more sustainable and economically viable unpaved road sections [39, 41]. Ingle and Bhosale [42] conducted a full-scale laboratory accelerated pavement test on unreinforced and geotextile reinforced unpaved road using 35000 loading cycles of standard axle load. Based on the change in vertical stresses recorded at various radial distances from the loaded section, mobilization of membrane action of geotextile was recognized to initiate after nearly 26000 cycles. Similar observation was made by Demir et al. [43] based on large-scale tests for geogrid-reinforced unpaved roads. With the aid of laboratory-scale CBR tests, Singh *et al*. [44] critically illustrated the usage of single and dual layers of different types of geosynthetics (Glasgrid, Tenax 3D grid and Tenax multimat), along with their positioning, on the enhancement of CBR of unreinforced sections. Calvarano *et al*. [14] conducted parametric study to give the limiting criteria of determining the base thickness of geogrid-reinforced unpaved roads. The work was further extended in a bi-dimensional finite element analysis framework (using FE software ABAQUS) to understand the performance of geogrid reinforced unpaved road under repeated loading [16]. Han *et al*. [45] conducted cyclic shear test to elucidate on the reinforcing mechanism of geogrid in unbound granular base in terms of the resilient shear modulus acting as an indicator to the interlocking mechanism between geogrid and aggregates. Based on laboratory plate load tests and traffic load tests, Khoueiry *et al.* [46] also highlighted the contribution of geogrid reinforcement in arresting the rut depths and enhancing the serviceability of unpaved roads. Based on moving wheel load tests, Singh *et al.* [19] conducted field tests with moving wheel load tests to evaluate the efficiency of geosynthetic (geogrid and geotextile) reinforced unpaved test sections constructed on subgrades with CBR less than 3% in terms of TBR and performance index. It was elucidated that separation action also plays an important role in reducing rutting in granular soil [19, 32]. Biswas *et al.* [47] conducted a series of repeated wheel load tests to investigate the behaviour of bamboo and jute geocell reinforcements on unpaved roads constructed with comprising an unbounded layer made of different materials (sand, crushed aggregate and recycled asphalt pavement). Considering a rut depth of 50 mm, extensive increase in the TBR was noted when the geocells were accompanied by an inclusion of basal geosynthetics.

It can be noted that most of the researches in the domain of unpaved roads has are concentrated to experimental investigations, either laboratory-scale or full-scale sizes. The published literature has successfully elucidated the benefit of utilizing geosynthetics as reinforcement in unpaved roads in order to increase the resilience and sustainability of the constructed stretches [48, 49]. However, in comparison, the study of reinforcing mechanism of geotextiles and geogrids in controlling the individual and coupled deformation of components of an unpaved road structure through numerical modeling and simulations are still limited and can further be investigated. More studies related to mechanism-based behavior of unreinforced or reinforced unpaved roads can help elucidating the intricate functional mechanisms of geosynthetics on reducing permanent deformation or rutting in unpaved roads. Most of the earlier analytical and numerical researches on unpaved roads were carried out considering the undrained cohesion as the only strength parameter of the soil subgrade [22, 23, 26, 27, 30, 31]. However,

depending on the drainage state (undrained, partially drained or fully drained) of the marginalized soil subgrade, strength parameters can be characterized by both cohesion (c) and angle of internal friction (φ). The consideration of conservative strength magnitude leads to over-estimated assessments of aggregate thickness that might not be practically required owing to actual strength of soil subgrade available at the site. Conventional limit equilibrium based analytical formulations for unpaved roads are generally prescribed following the two-dimensional (2D) plane-strain assumption, wherein the vehicular load is considered a strip load acting along the road. The wheels are assumed to always travel along the same section of the road such that every cross-section of the road receives the same magnitude of load and undergo same magnitudes of deformation [22, 50, 51]. However, in reality, the actual problem presents a hybrid scenario, wherein the operation placement of aggregate on the soil subgrade follows a 2D plane-strain problem, while the imposition of vehicular traffic is a three-dimensional loading scenario. Hence, for a better insight, the scenario of unpaved road design can be considered judiciously as a 3D problem. Considering all the factors, a 3D analytical expression is developed to determine the thickness of unpaved road constructed on marginalized cohesive-frictional (c-φ) soil subgrade. Then a finite element (FE) analysis of unreinforced, as well as geotextile reinforced, unpaved road constructed on marginalized soil subgrades is conducted. In this regard, the soil subgrade is considered to be specifically weak to exhibit the full benefit of using geosynthetics. At first, FE analysis of unreinforced unpaved road for quasi-static loading is carried out. Under different operational conditions, the deformation of individual layers of unpaved road are investigated. Further, a single layer of geosynthetic is introduced as a reinforcement at the aggregate-subgrade interface to investigate the influence of its tensile stiffness in arresting and reducing the stresses and strains developing in the unpaved road system. Further, the application of geosynthetic in reducing the rutting in the unpaved road system developed due to repetitive vehicular loading is also discussed, and the benefits of using geosynthetic as reinforcement to construct an economical and sustainable unpaved road structure is elucidated. In this regard, the novelty of the present work lies in the concept of using coupled stress-deformation approach to formulate a design principle of unpaved roads by considering its individual components as deformable bodies.

2. Analytical expression to assess thickness of aggregate layer based on three-dimensional load dispersion

Over the years, various researchers have proposed design methods to determine the thickness of unpaved road. Giroud and Noiray [22] pioneered the development of a design method to estimate the thickness of aggregate layer for unpaved roads that is based on a load dispersion mechanism through the aggregate layer overlying a purely cohesive subgrade soil. Such design of unpaved roads used CBR as an indicator of the undrained shear strength or undrained cohesion of soil subgrade [22]. However, the estimation of CBR disregards the frictional strength of subgrade material. Thus, the overall design based on CBR value is conservative, thereby expectedly increasing the aggregate thickness of unpaved roads. The design method by Giroud and Noiray was further improved by Meena *et al*. [50] considering unpaved roads resting on a generalized c-φ soil subgrade that is encountered more frequently in the field conditions. The developed expression was also based on a quasi-static analysis using limit equilibrium (LE) approach for a 2D plane-strain problem. Quasi-static analysis represents worst case scenario, wherein a vehicle is considered to be static for a significantly long time and, as a result, there is a complete stress transfer through the interaction of the vehicle tire with the aggregate layer [22]. As mentioned earlier, a 3D stress distribution approach would be better suited for assessing the thickness of aggregate layer required under a quasi-static scenario. A dual wheel vehicular axle load [22, 30] is considered in the present study,

wherein each dual-wheel carries half of the axle-load (i.e. $P/2$). The load is transferred to the aggregate layer through the contact area of the dual wheel, whose equivalent dimensions are represented by B and L, respectively, thereby the equivalent contact stress transferred at the tire-aggregate interface is expressed as $q_{eq} = P/(2BL)$. Further, as shown in Fig. 1, the generated contact stress on the surface of aggregate layer (q_{eq}) is assumed to follow a pyramidal stress distribution through the depth of the aggregate layer (h) and spread over a dispersed area at the aggregate-subgrade interface, having a dimension of $B'(= B + 2h\tan\alpha) \times L'(= L + 2h\tan\alpha)$. The required aggregate thickness is determined by equating the stress generated at the aggregate-subgrade interface to the allowable subgrade strength of the soil subgrade. It is to be further noted that at the aggregate-subgrade interface, the overburden stress due to the aggregate ($\gamma_{agg}h$) is omnipresent, and it gets added to the dispersed wheel stress to generate the total stress at the aggregate-subgrade interface (q).

For an axle load P, using the stress equilibrium, the stress generated at the aggregate-subgrade interface is expressed as follows:

$$q = \frac{0.5P}{B'L'} + \gamma_{agg}h; \quad B' = B + 2h\tan\alpha; \quad L' = L + 2h\tan\alpha \tag{1}$$

The generated stress is equilibrated with Terzaghi's (1943) proposition to determine the allowable bearing capacity for a shallow footing resting on a c-φ soil subgrade, which is expressed as:

$$q_{all} = \frac{c_{sub}N_cS_c + \gamma_{agg}hN_qS_q + 0.5\gamma_{sub}B'N_\gamma S_\gamma}{\text{FoS}} \tag{2}$$

where, $\gamma_{agg}h$ is the overburden pressure on the subgrade due to aggregate layer and FoS is the factor of safety. The unit weight of soil and aggregate are γ_{sub} and γ_{agg} respectively. As both have nearly similar value, henceforth γ would be used to represent either of the densities. N_c, N_q, N_γ are the bearing capacity factors which depends on the angle of internal friction of the soil (φ_{sub}). S_c, S_q, S_γ are the shape factors which value depends on the equivalent contact dimensions (B' and L') of the wheel load and α is the stress distribution angle $\left(\alpha = \pi/4 - \varphi_{agg}/2\right)$. Equation 3 gives the final expression to determine the aggregate thickness (h) of unpaved road resting on c-φ soil subgrade

$$\frac{0.5\text{P}}{\left(B + 2h\tan\alpha\right)\left(L + 2h\tan\alpha\right)} + \gamma h = \frac{c_{sub}N_cS_c + \gamma hN_qS_q + 0.5\gamma B'N_\gamma S_\gamma}{\text{FoS}} \tag{3}$$

3. Numerical Methodology

Equation 3 gives the expression of required thickness of aggregate layer based on a LE approach, which considers the individual components of unpaved road structure to be rigid and non-deformable. However, due to the booming industrialization, the availability of good quality construction materials to be used in unpaved road is gradually decreasing. Furthermore, owing to site-specific constraints, many a times, the unpaved road system has to be constructed on marginalized soil subgrades. For such unpaved roads, deformation arises outright during the initial construction and might exhibit operational failures, especially (i) failure or permanent deformation of weak subgrade layer due to the weight of stacked unbounded and poorly-graded coarse aggregate layer during their laying operation and (ii) failure within aggregate layer due to the stresses developed by quasi-static vehicular loading and long-term deformation in the form of rutting due to repeated vehicular loading. Thus, deformation

under different operational conditions becomes a guiding factor for the design of unpaved road [24, 52]. However, LE based design of unpaved road fail to highlight these phenomena. In this regard, a FE based design, based on coupled stress-deformation approach, incorporating operational loading conditions seems prudent for a sustainable and economically viable design of unpaved road system.

Accordingly, a FE-based design of unpaved road resting on generalized c-φ soil subgrade is conducted. For the present research work, the numerical modelling software PLAXIS 3D is used to simulate the unpaved road system. Figure 2 depicts a typical geometry of the unpaved road, comprising the overlying aggregate and underlying soil subgrade layers. Given the specific magnitudes of the contributing parameters, the thickness of the aggregate layer is adopted as per the solution of Equation 3. To avoid any slope failure along the sides of the aggregate, the slope of the aggregate layer is maintained to a value of 3H:1V (or 4.5H:1V for higher axle loads). The width of the road is considered to be 7 m. The vehicle, comprising the front axle wheels (FAW) and rear axle wheels (RAW), is placed along the center-line of the road. Uniformly distributed vehicular load under the wheels, acting over contact width, are considered on the surface of the aggregate layers; the wheels being separated from each other as per the chosen axle width. The soil subgrade layer is considered homogeneous and semi-infinite, the dimensions of which are judiciously decided such that the lateral and bottom boundaries do not intersect or influence the development of stress, strains or deformations in the subgrade that are originated and propagated from the aggregate layer. Along the lateral boundaries of the subgrade layer, horizontal fixities are provided, while the bottom boundary of subgrade is fully fixed against both horizontal and vertical displacements. The effect of water table is not considered in the present study, and hence drained conditions is adopted for the numerical analyses.

Both the subgrade and aggregate layer are represented using Mohr–Coulomb (M-C) model that follows a linear elastic – perfectly plastic constitutive relationship. This model allows elastic behaviour up to the yield limit, beyond which plastic flow occurs under constant stress. The Mohr-Coulomb yield point is defined by the friction angle of the material [53, 54]. Although the M-C model considers the variation of material strength with lateral confinement (wherein the material strength increases with stress level), it does not consider the variation of elastic modulus with stress levels [55]. The model is capable of capturing the hysteretic loading-unloading behaviour if plasticity occurs, i.e. if the yield stress level is reached [56, 57]. The loading, unloading and reloading modulus remain constant (equal to chosen Young's modulus) for each cycle of stresses. Each cycle of loading-unloading is characterized by a residual strain or residual deformation, with a portion of total strain being recovered due to the elastic unloading. Hence, in case of repetitive loading, the M-C model is capable of producing accumulative settlement, provided that at each loading and reloading cycles, the yield stress is attained. In such case, for repetitive loading, the accumulation of settlement would be noticed after each loading cycle, as depicted in later parts of the present study.

The constitutive behaviour of Mohr-Coulomb model is controlled by five input parameters, soil elasticity and stiffness represented by Young's modulus (E) and Poisson's ratio (ν), while the strength being represented by angle of internal friction (φ), cohesion (c) and angle of dilatancy (ψ) for soil plasticity [58]. For the present study, dilatancy is not considered. Table 1 reports the typical material properties used in the FE models developed to investigate the stress-deformation response of unpaved road constructed on weak or marginalized soil subgrade

and subjected to quasi-static or quasi-dynamic loading scenarios. It is to be noted that Table 1 specifically reports the magnitudes of unit weight and stiffness parameters that are adopted in the present study. The adopted magnitudes conform to the reasonable range of the corresponding parameters that are encountered in the construction materials of such unbounded roads and reported in relevant literature [50, 59]. It is also to be noted that the specific strength parameters of the marginalized subgrade (cohesion, c_{sub}, and angle of internal friction, φ_{sub}) are not mentioned in Table 1. In the latter half of the manuscript, Section 5.1 and Section 5.2 utilizes different magnitudes of the strength parameters to elucidate the influence of quasi-static and quasi-dynamic loading scenarios, respectively, on the response of FE model. Thus, the specific magnitudes of the shear strength parameters are explicitly mentioned thereof and, hence, is not mentioned in Table 1 as typical magnitudes. For the subgrade and aggregate layers, the unit weight (γ) is kept same owing to the fact that the unit weight of soil and locally available aggregates are mostly similar and that slight variations in this parameter does not significantly affect the deformation response of the unpaved road system [50]. Two different vehicular axle loads of high magnitudes, 360 kN and 190 kN, are used in this study for quasi-static and repetitive vehicular loading analyses [22, 27, 60]. The high axle loads considered here are common for heavy haul caterpillar dump trucks [61] and are specifically considered for the present study to distinctively elucidate the robustness of the FE-based design algorithm described in the latter sections of the manuscript.

A mesh convergence study is carried out for a particular model configuration to identify the sensitivity of the FE model to the variation in mesh size. In PLAXIS 3D, finite element meshes of various element sizes can be generated by taking into account the soil stratigraphy as well as all objects, loads and boundary conditions. It was exhibited by Sarma and Dey [51] that for two-dimensional modeling, a mesh convergence was achieved for 'medium' mesh with an average element size (AES) of 1.2 m (approximately). Following the same, in the present study, mesh convergence is conducted with 'medium'-sized mesh having different coarseness factor to generate larger density of mesh element. Figure 3 represents the outcome of the mesh convergence study conducted for the model. It is observed from the output results that for 'medium' mesh size with a coarseness factor of 0.25, thereby yielding and AES of 0.0056 m, the convergence has been achieved; beyond which reduction in mesh size did not substantially alter the results. Furthermore, in areas of large stress concentrations, additional local mesh refinement is also provided at the aggregate-subgrade interface and corners of the aggregate layer.

3.1 Validation study

It is important to conduct a validation study to understand the capability of the developed FE methodology in capturing the stress-deformation response from a chosen constitutive model. Such validation studies are conducted primarily to gain confidence on the developed numerical model such that it can represent the experimental findings to an acceptable extent. In this regard, a suitable experimental investigation is chosen in similitude to the considered problem, and the suitability of the developed FE model and the adopted constitutive relationships is judged based on the similarity in the outcomes from the numerical analysis and experimental investigations. Once the numerical model is validated, the same model itself can be further used, especially for parametric investigations. However, it is not mandatory to proceed with the validated model for further research. If the suitability of the numerical methodology and constitutive relationships is already established through the validated model, the geometrical dimensioning and the material properties of the validated model can be altered to suit the

actual research problem, as long as the relative geometrical configuration and constitutive behaviour of the individual components of the FE model is not altered. In the present study, the FE model of the unpaved road comprises two layers (aggregate layer overlying the subgrade layer) with loading from dual wheel (representing the quasi-static vehicular load) on an equivalent rectangular tire-contact area over the aggregate layer (as shown in Fig. 2). In absence of an exact experimental representation of quasi-static loading on an unpaved road system, for the present study, the validation is carried out with respect to an experimental investigation by Roy and Deb [62]. The stated experimental investigation [62] deals with the interference effect of two closely-spaced identical footings resting on granular fill of limited thickness over soft clay and, accordingly, a corresponding FE model is developed (as shown in Fig. 4). Both the FE models, i.e. one that used for unpaved roads (Fig. 2) and the one used for validation study (Fig. 4), have the same physical structure of double-layered soil system with a granular layer overlying the marginalized or soft soil layer. For both the models, closely spaced interfering rectangular areas placed over the granular layer subjected to uniformly distributed loads is considered. For both the models, the granular fill and soft clay is represented by the Mohr-Coulomb constitutive relationship. Hence, in light of these similarities, if the FE model for validation study (Fig. 4) shows agreeable results with the experimental investigations, the FE model unpaved road (Fig. 2) can also be considered validated as long as it follows a similar relative geometrical configuration and utilizing the same constitutive relationship for the different components of the numerical model.

Out of all the experiments conducted by Roy and Deb [62], the following information are used for the validation study: rectangular footing of dimensions 75(b)×150(l) mm (width × length), center-to-center spacing of the footing (S) as 2.0b (= 150 mm), and thickness of the top layer (d) being equal to 0.75b. Figure 4 shows the corresponding FE model, whose material properties are listed in Table 2. The experiment by Roy and Deb [62] was conducted within a steel tank. Hence, as per the experimental set up, in the numerical model, the bottom boundary of the soft clay layer is fully fixed against vertical and horizontal displacements, while, along the lateral boundaries, only horizontal fixities are provided. As per the information from experimental investigations, the soft clay was maintained at an undrained condition, while the presence of sand bed provided a drained condition in the overlying layer; the same is maintained in the numerical model. The loading rate in the numerical model is maintained at 2 mm/min in conformity to the rate of loading in the experimental investigation. In the experimental investigation, settlement is measured through dial gauges positioned at the edges of the footing. In conformity, in the FE model, the closest relevant displacement nodes are selected on both sides, as well as in the center, of the footings. For the selected nodes, the output result of the FE analysis (in the form of bearing pressure vs settlement ratio) is compared to that obtained from the experimental observation. Figure 5 denotes the agreeable similarity between the responses; for a maximum settlement ratio of 26.5%, the bearing pressure values from FE and experimental results are 51.91 kPa and 51 mm respectively. A minor dissimilarity can be noted between experimental and FE results (with an average deviation of 5-8% over the plot), which is possibly due to the idealization of the stiffness of experimental sand bed being considered constant in Mohr-Coulomb constitutive model, whereas the actual experimental programs generally reflect a pressure-dependent stiffness. However, such dissimilarity remains existent and are well within the tolerable limit (<10%). Based on these observations, the corresponding FE model (Fig. 4) can be considered validated, and in line to the previous discussion, the FE model

for the unpaved roads can also be considered validated and the same is utilized for further studies reported in this paper.

4. Coupled Stress-Deformation based Design Methodology for Unpaved Roads

4.1 Operational failure conditions and limiting cohesion

As Equation 3 is developed based on LE method, the aggregate and subgrade layer is considered non-deformable. However, in reality, a weak marginalized subgrade might not provide the required bearing resistance during the laying process of stacked unbounded aggregate itself. This would be manifested by the subsidence of the aggregate within the subgrade layer. This leads to a loss in design thickness necessitating additional aggregate placing and incurring higher expenditures. Similarly, in the absence of finer binding material within the cluster voids, aggregate can undergo prevalent punching failure under the vehicular loading, especially at the edges of the tire contacts. These two stated failures constitute the 'operational failures' during the construction and service life of the unpaved road, which is not incorporated in the LE based analytical solutions. In this regard, the strength parameters of the aggregate and soil subgrade needs to be improved to counteract such operational failures. Accordingly, the expressions for the minimum cohesion, required individually by the subgrade and aggregate, are determined from limit analysis. The minimum cohesion required to tackle operational failure are further incorporated to propose the coupled stress-deformation based approach for FE model of unpaved roads.

4.1.1 Expression for limiting cohesion in subgrade layer required to sustain aggregate loading

The subgrade should be strong enough for sustaining the aggregate load during its placement. Hence, following Terzaghi's bearing capacity formulation for an analogous surface strip load resting on supporting soil [63], the expression for minimum cohesion required by subgrade under operational condition is developed by equating the aggregate stress (γh) to the allowable bearing capacity of the subgrade. The same is expressed as follows:

$$\gamma h = \frac{c_{sub-\min} N_c S_c + 0.5\gamma B' N_\gamma S_\gamma}{\text{FoS}} \tag{4}$$

where, $c_{sub\text{-}min}$ is the minimum cohesion required in soil subgrade, and rest of the parameters are same as described in Equation 2.

4.1.2 Expression for limiting cohesion in aggregate layer required to sustain quasi-static vehicular loading

The aggregate layer under quasi-static loading might experience punching shear failure from the concentrated stresses developed at the sides of the wheel. In such case, the stress concentration under edges of the tire contacts should be dispersed to a magnitude lower than the allowable bearing capacity of the aggregate alone. Hence, following Terzaghi's bearing capacity formulation for a surface strip load resting on supporting soil [63], the expression for minimum cohesion required by the aggregate ($c_{agg\text{-}min}$) under operational condition can be expressed as

$$\frac{P}{2BL} = q_{eq} = \frac{c_{agg-\min} N_c S_c + 0.5\gamma B N_\gamma S_\gamma}{\text{FoS}} \tag{5}$$

where, $c_{agg\text{-}\min}$ is the limiting cohesion required to prevent punching shear failure in the aggregate layer due to the imposed quasi-static vehicular loading. The corresponding bearing capacity factors are to be determined based on

the friction angle of the aggregate material. Similarly, corresponding shape factors are determined based tire contact dimensions of the wheel load.

4.1.3 Additional cohesion requirement of subgrade considering deformability of aggregate and subgrade

In the previous sub-sections, separate expressions are developed to determine minimum cohesion required by the subgrade and aggregate to ensure their individual operational stability against failure. However, in practical scenario, the stress-deformation mechanism of the unpaved road system will be coupled and the subgrade would be a deformable medium; thereby, the stability of individual layers would be affected by the secondary stress transfers through stress-deformation interaction between the layers. Since the aggregate layer is already ensured to be stable under vehicular load, further failure in this layer under operational condition can only be triggered because of the deformable subgrade. Hence, in such situation, the cohesion of the subgrade needs to be further modified to arrive at a minimum value ($c_{sagg\text{-}min}$) that would render the subgrade enough bearing strength to sustain the overall imposed stress, inclusive of the secondary stresses. In the next section, implementation of such expressions is discussed. Such improvement in strength of the subgrade is possible by adopting proper ground improvement techniques, wherever necessary, although the choice of the ground improvement techniques is beyond the scope of the present study.

4.2 Design Methodology for Unreinforced Unpaved Road Design

Following are the step-by-step design procedure of unreinforced unpaved road structure based on coupled stress-deformation approach. For easy visualization, Fig. 6 exhibits the developed algorithm in the form of a flowchart.

Step 1. Make a preliminary assessment of the required aggregate thickness (h) based on Equation 3.

Step 2. Develop the FE model in PLAXIS 3D using aggregate thickness assessed in Step 1. The shear parameters (c_{sub}, $\varphi_{sub;}$ and φ_{agg}) for subgrade and aggregate layers is to be kept same as that used in the analytical expression used for assessing the aggregate thickness (Eqn. 3). The values of other model parameters such as modulus of elasticity (E), Poisson's ratio (ν), unit weight (γ) are adopted as per field specifications.

Step 3. The simulation of the FE model developed in Step 2 is undertaken to investigate the operational instability of the subgrade solely due to aggregate loading. If the operational stability is not jeopardized, consider $c_{sub\text{-}min}$=c_{sub} and continue to Step 6. If the FE model exhibits stress-based failure in the subgrade, continue to Step 4.

Step 4. Assess the limiting magnitude of cohesion ($c_{sub\text{-}\min}$) required in the subgrade layer (as per Eqn. 4) to sustain the operational aggregate loading.

Step 5. Using the $c_{sub\text{-}min}$ value obtained in Step 4, analyse the FE model developed in Step 2 to ascertain the operational stability of the subgrade under aggregate loading. If the subgrade remains stable under the aggregate load, continue to Step 6. If the subgrade still portrays failure, repeat Step 4 to re-estimate $c_{sub\text{-}min}$ with higher FoS.

Step 6. Reform the FE model by incorporating $c_{sub\text{-}min}$ as the cohesive strength parameter for the subgrade (obtained in Step 5) along with the friction strength parameter of the subgrade (φ_{sub}). Investigate whether the aggregate layer (with strength parameter adopted in Step 1 or Step 2) is operationally stable and able to sustain the punching stress concentration imposed by the quasi-static vehicular load.

Step 7. If operational stability of aggregate layer is ensured, the design of unpaved road is deemed complete with φ_{sub} and $c_{sub\text{-}min}$ as the shear strength parameters for the subgrade, and φ_{agg} as the shear strength parameter for the aggregate.

Step 8. If the aggregate fails under the imposed vehicular load, determine the minimum value of cohesion required ($c_{agg\text{-}min}$) in the aggregate using Equation 5.

Step 9. Analyse the reformed FE model developed in Step 6 (already having φ_{sub}, $c_{sub\text{-}min}$ and φ_{agg}) by incorporating $c_{agg\text{-}min}$ as limiting aggregate cohesion to reassess its operational stability.

Step 10. If the aggregate still exhibits operational instability, considering a higher FoS. Further, proceed to Step 9 to include the re-estimated $c_{agg\text{-}min}$ in the reformed FE model that is already incorporating the φ_{sub}, $c_{sub\text{-}min}$ and φ_{agg} (from Step 6). If the reformed FE model with higher magnitude of $c_{agg\text{-}min}$ in aggregate layer exhibits operational stability, proceed to Step 11; else, repeat Step 10 again by heuristically and iteratively enhancing $c_{agg\text{-}min}$ to a higher value.

Step 11. If the aggregate does not exhibit stress-based failure under imposed load and that the operational stability of the aggregate is ensured, the strength parameters of unpaved road system is finalized to φ_{sub} and $c_{sub\text{-}min}$ as the shear strength parameters for the subgrade, along with φ_{agg} and $c_{agg\text{-}min}$ as the shear strength parameter for the aggregate. Even after achieving operational stability, it is necessary to check whether the reformed FE model exhibits failure in the subgrade due to the secondary stresses generated in the subgrade for simultaneous aggregate and vehicular loading. Thus, the unpaved road system is further checked for failure under secondary stresses.

Step 12. If no secondary stress-based failure is noticed, the design of unpaved road system is deemed complete with the strength parameters finalized and mentioned in Step 11.

Step 13. Any instability in the subgrade arising due to the secondary stresses (as in Step 11) can be tackled by heuristically and iteratively increasing the value of $c_{sub\text{-}min}$ to a modified higher value ($c_{sagg\text{-}min}$).

Step 14. The FE model is reanalysed with $c_{sagg\text{-}min}$ as modified cohesion of the subgrade to reconfirm the stability of the system against secondary stresses.

Step 15. If the stability against secondary stresses is achieved, the design of unpaved roads is deemed complete with the strength parameters of unpaved road system is finalized to φ_{sub} and $c_{sagg\text{-}min}$ as the shear strength parameters for the subgrade, along with φ_{agg} and $c_{agg\text{-min}}$ as the shear strength parameter for the aggregate. If the stability is yet to be achieved, repeat from Step 13.

4.3 Design Methodology for Reinforced Unpaved Road

4.3.1 Quasi-static loading condition

In the previous part of the study, it is understood that unreinforced unpaved road built on soft soil subgrade is susceptible to deformation under operational conditions. To counteract such problems, ground improvement techniques need to be implemented to ensure stability of the unpaved road system. As mentioned earlier, traditional ground improvement techniques are costly and require lots of manpower or automated resources (for soil replacement, compaction etc). Use of geotextile as reinforcement is a viable alternative for an economic and sustainable solution to the problem. Geotextiles are planar members that can sustain and induce tensile force within the compressible soil. Hence, in this part of the study, the FE model developed for unreinforced unpaved road is improvised to include a single layer of geotextile at the aggregate-subgrade interface. In PLAXIS 3D, 6-noded triangular geosynthetic surface elements are available for this purpose. The geosynthetic element is represented by elastic and isotropic material behavior. For an elastic geotextile, the basic material property is its axial stiffness (*EA*). The axial stiffness value is varied between 200-1000 kN/m (within the range for woven geotextiles available in practice for road construction projects) to understand the benefit imparted by geotextiles with different stiffness values [22, 45]. For proper bonding between the geosynthetic and the surrounding soil, interfaces are provided on both sides of the geosynthetic. Figure 7 shows the FE model reinforced unpaved road, wherein it can be noticed that the geosynthetic is placed at the interface of aggregate and subgrade. Hence, in the numerical model, two interfaces are created; one between aggregate and geosynthetic (i.e. above the geosynthetic) and the other between geosynthetic and subgrade (i.e below the geosynthetic) (Fig. 7). The strength of the interface is governed by the strength reduction factor (R_{inter}) value, signifying the roughness of interaction between two dissimilar materials while they are shearing to each other. Generally, R_{inter} value ranges between 0 (zero) to 1 (one). A value of R_{inter} = 0 signifies the interface to be smooth and full slippage is allowed, while a value of 1 (one) emulates perfect bonding through a rough interface where no slippage is allowed. In the present study, the interface is provided between two materials i.e. soil subgrade and geotextile and that between geotextile and aggregate. In most geotechnical engineering problems involving shearing of one medium over the other, the magnitude of R_{inter} is maintained less than one as one material is allowed sliding over the other. For example, in slope stability problems involving soil-geosynthetic interfaces, it is a common practice to consider the critical strength at the interfaces, and hence R_{inter} value can range between 0.4-0.7 [64, 65]. However, in the present study, the aggregate-geosynthetic and geosynthetic-subgrade interface is meant to bear the compressive loads and is expected to undergo minimal shearing induced slippage along the length of the geosynthetic. Further, the aggregate-geosynthetic interface is supposed to be quite rough so that slippage is prevented and the membrane action of the geosynthetic is triggered from stretching of the geosynthetic owing to the lateral stresses transferred from the aggregate layer to the geosynthetic interface. As the aggregate and geosynthetic is considered in perfect bonding to each other without any slippage, R_{inter}=1 is assumed in the present study.

As discussed in Section 4.2 for unreinforced unpaved roads, in Steps 3-5, the subgrade is considered failing under aggregate loading. Further, in Step 11, the subgrade again is considered for failure due to the secondary stresses generated by simultaneous aggregate and vehicular loading. Instead of adopting a conventional ground improvement technique to induce modified strength parameters for subgrade and aggregate to ensure the stability of unpaved road, incorporation of geotextile layer is considered and the FE model is analysed in the corresponding steps for different operational conditions. However, yet there might be some cases of extremely weak subgrade wherein even after incorporating geotextiles of higher stiffness, the subgrade might show signs of impending failure; in such cases, some ground improvement technique needs to be inadvertently adopted to ensure stability of the reinforced unpaved road system.

4.3.2 Repeated Loading condition

In the previous section, FE analyses were adopted to conduct quasi–static analysis for designing and assessing the performance of unpaved roads. Although quasi-static analysis represents a worst-case scenario, in actual field condition, load repetition effect due to successive vehicular passages are prevalent in actual field situation. Therefore, a FE-based study is conducted to decipher the effect of vehicular load repetition on the behaviour of unreinforced and reinforced unpaved road. The problem is tackled as a quasi-dynamic problem. In this case, the actual time-dependent spatial movement of the vehicle is represented in terms of the axle load repetitions at specific intervals of time. This is conveniently represented by a triangular or Haversine loading of specific duration (denoting the passage time of the vehicle through the specific section of the road) and repeating at a specific time interval (denoting the passage of successive similar vehicles). In such consideration, the main parameters of load repetition that are considered comprise the equivalent contact stress at the tire-aggregate interface ($P/2BL$), number of load passes (N), time gap between the arrival and departure of the vehicle through a road section (t') and time interval between two consecutive passes (Δt). Following such consideration, the input signal of quasi-dynamic vehicular load is considered to be triangular or Haversine in nature to give a realistic view of the multi-vehicular passage through a common section [7, 42, 43, 52, 64-66]. The two arms of the triangular/Haversine input signify the approach (rising arm of the loading) and departure (falling arm of the loading) of a vehicle through the particular section of the road. In the present problem, as shown in Fig. 8, the quasi-dynamic load is applied through dynamic load multipliers repeated at regular time interval (Δt) of 2 s. The approach of a vehicle (denoted by the rising arm of the triangular input) takes place over a time span of 0.1 s, following by its departure (denoted by the rising arm of the triangular input) from the same section in the next 0.1 s. Hence, the overall time duration of the passage of vehicle over a particular section (t') is 0.2 s. Figure 9 depicts a typical displacement profile observed beneath the wheel for a single passage of the vehicle. It can be noticed that during the interval 0.2-0.4 s, the displacement follows the haversine triangular pattern in congruence to the applied triangular load. Furthermore, interestingly, as the vehicle departs, an elastic rebound is observed for around 1.2-1.3 s, beyond which the displacement culminates to a residual magnitude. Hence, in the present study, the next vehicular pass is considered at a time interval after the completion of the elastic rebound, and accordingly a conservative resting time interval of 2 s is adopted before the application of next passage of the similar vehicle. However, any other time interval could have been also considered depending upon the actual traffic passage through the road section. In the present study, identical vehicle passages are considered, and the influence of mixed mode vehicular configuration is kept out of scope from the analyses.

In this study, influence of repetitive loading conditions on unpaved road structure are investigated for both unreinforced and reinforced scenarios. The development of FE model of unpaved road is similar to the quasi-static loading condition discussed in a preceding section. The main difference remains in the input of the repeated loading that is described in the previous paragraph (as in Fig. 8). Initially the response of unreinforced FE model of unpaved road is observed under repetitive loading for a particular material model parameter. If the unreinforced unpaved model shows signs of failure due to the rutting at the surface of the aggregate layer due to repeated loading, a geotextile layer is introduced to develop the FE model for reinforced unpaved road and the same is subsequently analyzed.

5. Results and Discussion

This section gives the FE output results of unreinforced as well as reinforced unpaved road under quasi-static and repeated loading conditions.

5.1 Quasi-static loading

In this section, an exemplified finite element-based design of an unpaved road system subjected to quasi-static loading condition is discussed. The parametric values for the analysis of the parent model considered herein are as follows: P = 360 kN, P_c = 600 kPa, c_{sub} = 1 kPa, φ_{sub} = 5° and φ_{agg} = 25° and FoS = 1. In the present study, a dual wheel system truck is considered as they are more prevalent than single wheel version on unpaved roads. In a dual wheel system, it is considered that the soil in-between the tires get mechanically associated with the wheels. As it is understood that the mechanically associated soil or aggregate between the tires would not undergo failure, they represent a composite or equivalent contact area that is larger than twice the actual contact area of each tire [22, 50]. Accordingly, considering on-highway vehicles, the width of the equivalent contact area is given as $B = \sqrt{P / P_c}$ and $L = B/\sqrt{2}$; for off-highway vehicles the same is denoted as $B = \sqrt{P\sqrt{2} / P_c}$ and $L = B/2$ [22]. Accordingly, in the present study, based on the chosen magnitudes of P and P_c, the equivalent contact dimensions are estimated as B = 0.77 m and L = 0.55 m. The strength properties of subgrade and aggregate layers are considered to be minimum such that the individual layers undergo deformation and the minimum cohesion-based design is illustrated through the FE-based design methodology. Later on, the benefit of incorporating geosynthetics in the parent model are exhibited

5.1.1 Outcomes from a typical FE-based simulation for unreinforced unpaved road

As discussed in Section 4.2, a step-by-step design methodology of unreinforced unpaved road structure is conducted. The outcome of the design is as follows:

- **Step 1**: Based on the parametric data and following Equation 3 (with FoS=1), the thickness of aggregate layer (h) is preliminarily assessed to be 1.21 m. The assessed aggregate thickness is quantitative agreement to the thickness required if the weak subgrade was characterized only by undrained cohesive strength [22].
- **Step 2**: A FE model is developed with the thickness of aggregate layer obtained in Step 1. The material properties of the model are kept the same as mentioned above and the side slopes of the aggregate layer are maintained to 3H:1V.

- **Step 3**: For the unpaved road model developed in Step 2, operational stability of the subgrade is checked under the aggregate loading. Since the unpaved road system has uniform cross-section along the length of the road, following the plane-strain condition, the output results along a perpendicular section gives representative observation for the whole length of unpaved road. Figure 10 shows that under aggregate loading, significant deviatoric strains have developed, as manifested by the slip lines propagating through the aggregate layer to the subgrade layer. The observation indicates that the subgrade is not sufficiently strong to bear the aggregate loading and that it fails even due to the mere laying of the aggregate, thereby necessitating enhancement in its strength properties.
- **Step 4**: From Step 3, it is understood that the strength of the subgrade layer is required to be enhanced, which can be achieved by increasing the subgrade cohesion. Following Eqn. 4 and considering FoS=1, the minimum cohesion required in the subgrade layer to sustain the aggregate loading ($c_{sub\text{-}min}$) is assessed to be 1.88 kPa, which is marginally more than the initial value of c_{sub} = 1 kPa.
- **Step 5**: The FE model developed in Step 2 is analyzed with modified cohesion of subgrade i.e. $c_{sub\text{-}min}$ = 1.88 kPa. The output results shows that the strains are well captured and restricted within the aggregate layer (Fig. 11). The maximum value of total deviatoric strain obtained after improvement is 2.212×10^{-3}, which is nearly 100 times lesser than that observed in Fig. 10. These observations conclusively indicated that with improved cohesion, the subgrade is capable of bearing the operational aggregate load. Hence, $c_{sub\text{-}min}$ = 1.88 kPa is used in the subsequent analyses. This step reenacts the necessity to depend on coupled stress-deformation based finite element modeling to assess the operational response of subgrade under aggregate loading, which cannot be captured by LE methodology.
- **Step 6**: After ensuring the stability of unpaved road under aggregate load resting on the reformed subgrade, the FE model is analysed for the operational stability of aggregate layer under quasi-static vehicular load. It is observed that under vehicular load, the FE model simulation exhibited failure (Fig. 12). The output result indicates the development of punching shear failure mechanism within the aggregate layer due to the imposed wheel load. The strains are heavily concentrated within the aggregate layer and maximum at and around the edges of the wheels. Hence, it is understood that the chosen strength parameters of the aggregate layer are insufficient to prevent failure in aggregate layer due to the vehicular load. Hence, there is a necessity to improve the aggregate strength.
- **Step 7:** As the aggregate is not operationally stable under imposed vehicular loading, the necessary shear strength of the aggregate is not achieved, and hence the design is progressed to Step 8.
- **Step 8**: Following Equation 5 and with FoS=1, the strength parameter of the aggregate layer is further increased and the minimum value of cohesion required in the aggregate layer to sustain vehicular loading (c_{agg}-*min*) is determined to be 12.26 kPa. This can be achieved by introducing fines in the aggregate layer in a controlled manner.
- **Step 9**: Subjected to quasi-static vehicular loading, the FE model developed in Step 6 is further analysed with increased cohesion of aggregate (c_{agg}-*min*). It is observed from Fig. 13 that the failure in the aggregate layer is arrested by increasing the strength within the layer. As shown in Fig. 12, the strains developed are very negligible as compared to that developed in Step 6.

- **Step 12:** It can be noted from Fig. 13 that the total deviatoric strains are all concentrated within the aggregate layer itself. As there is no secondary failure encountered in the subgrade due to vehicular loading, the final design parameters for the complete stability of the unreinforced unpaved road under different stages of operation are φ_{sub} = 5°, $c_{sub\text{-}min}$ = 1.88 kPa, φ_{agg} = 25° and $c_{agg,\text{-}min}$ = 12.26 kPa respectively.

5.1.2 Outcomes from a typical FE-based simulation for reinforced unpaved road

A step-by-step design methodology of unreinforced unpaved road has been discussed in Section 5.1.1. In Step 3, it was observed that subjected to operational aggregate loading, the subgrade layer undergoes failure. In this regard, the strength parameter of the subgrade layer was increased to stabilize the system. Thus, for an unpaved road structure founded on deformable weak subgrade, additional ground improvement might be required to strengthen the unpaved road system under operational conditions. Depending upon the requirement, different types of traditional ground improvement techniques can be adopted based upon mechanical stabilization that aims to either compact the soils at the surficial regions or until larger depths. The depth of improvement required can be decided from the depth of slip lines formed in the subgrade. Surficial improvement techniques primarily involve compaction by the usage of different types of rollers and heavy weight drops or confides to soil replacement techniques where a portion of the existing subgrade soil can be replaced or blending by soils of better engineering characteristics. Soil improvement to larger depths are generally achieved by the advanced techniques of vibrocompaction, vibroflotation, blast-induced compaction or dynamic compaction accompanied by displacement piles. Soil stabilization using admixtures such as cement, lime, flyash, bitumen and fly-ash are other common adaptations [18, 67, 68]. The selection of ground improvement techniques depends on several factors such as type of soil, geographical structure, seepage conditions, degree of improvement required, availability of equipment and material, available construction time, durability and reusability of materials used, environmental conditions and, lastly, on the cost of project that might be a decisive one. These factors increase the overall cost of construction and consumption of raw materials for the construction. In this regard, inclusion of geosynthetics as reinforcement provides a more practical and cost-effective solutions to such problem.

In this regard, FE-based design methodologies were developed for reinforced unpaved roads under different operational conditions for quasi-static condition (as highlighted in Section 4.3.1). However, instead of increasing the cohesion of subgrade from 1 kPa to 1.88 kPa (Step 3 of Section 4.3.1), a layer of woven geotextile can be placed at the aggregate-subgrade interface to harness the benefits of introducing a tensile element in the deformable system. It has been shown by Meena *et al.* [50] that recognizable beneficial effects of geotextile in reduction of aggregate thickness is harnessed with those having tensile strength greater than 100 kN/m. Hence, following the recommendation, a geotextile having an axial stiffness of 400 kN/m is considered in the present study; geotextiles with these specified tensile strengths are commonly available as commercial products. It is observed that due to the inclusion of geotextile, the FE model does not undergo failure. Figure 14b shows the total deviatoric strain diagram after the inclusion of the geosynthetic layer. The maximum value is 0.06912, which is three times lesser than the maximum strain obtained in unreinforced case (Fig. 14a). With increase in tensile modulus, a geotextile is expected to sustain more stresses coming from the aggregate layer and should aid in reducing the stresses transferred to the subgrade; this phenomenon is pertinent to the ‘tension membrane effect’

displayed by a stretched geotextile. Hence, a geotextile of tensile modulus 1000 kN/m is further considered in the present study. Figure 14c shows the corresponding total deviatoric strain diagram after the inclusion of geotextile with higher tensile modulus. As illustrated in the Fig. 14c, the failure lines are almost diminished indicating a perfectly stable unpaved road structure. In similar unpaved road sections reinforced with different types of geosynthetics, Hufenus *et al.* [33] reported the development of strains approximately up to 0.8%, which provides conformity to the obtained results from the present numerical exercise; similar observation was also reported by Ingle and Bhosale [42] based on full-scale laboratory accelerated tests.

5.2 Repetitive Vehicular Loading

In the previous sections, step-by-step design methodology of unreinforced as well as reinforced unpaved road, based on quasi–static analysis, is illustrated. Although quasi-static analysis represents worst case scenario, in reality, for daily used unpaved roads founded on soft or weak soil subgrade, the overall performance of the road depends on the amount of vehicular load repetition. With gradual increase in the number of loads repetition, permanent damages in the unpaved road structure is generally observed, especially in the form of rutting. A finite element-based design of unpaved road is done to understand how rutting is developed with increase in the number of vehicular load repetition. Furthermore, the effect of geotextiles of various tensile modulus in arresting the rutting developed in the unpaved road section is also discussed.

The parametric values of the model analysed in this section are as follows: P = 190 kN, P_c = 600 kPa, B = 0.56 m, L = 0.4 m, c_{sub} = 10 kPa and φ_{agg} = 25°. In this model, the subgrade is considered to be comprising weak cohesive soil, while the aggregate is considered to made of purely granular material. Using Equation 3 and FoS=1, an unpaved road is modelled with an aggregate layer thickness of 0.1 m. The model is analysed for three different numbers of vehicular load repetition, i.e. 2 passes, 10 passes and 20 passes, respectively. The load repetition is described in the form of dynamic load multiplier as was typically illustrated earlier in Section 4.3.2.

5.2.1 Outcomes from a typical FE-based simulation for unreinforced unpaved road under repetitive loading

To observe the amount of rut developed due vehicular load, a perpendicular section (Section B-B) has been cut across the length of the road that passes through the edge of the rear axle wheels (Fig. 15a). Figure 15b provides a qualitative estimate of the amount of rutting developed at the surface of the unpaved road for three different numbers of vehicle repetitions, i.e. 2 passes, 10 passes and 20 vehicles pass, respectively, for rear axle wheel load. It is to be noted that the magnitudes of rutting shown in Fig. 15b are presented in exaggerated scale for intra-comparison and is not at the same scale of aggregate layer thickness. The vehicular loading induced rutting in unpaved roads on deformable subgrade is expressed as a combination of maximum settlement beneath the wheels and maximum heaving in-between the wheels [22, 35, 69]. It is observed from the Fig. 15b that the maximum heaving is near the edge of the vehicular load, while the settlement is maximum at the center of the vehicle tire. A recognizable rutting displacement is noted as the vehicle passes increase from 2 to 10, while the increase in rutting is not in significant magnitudes beyond 10 vehicle passes. With increase in the number of vehicular passes, the amount of rut increases significantly. The rut developed for the mentioned vehicle passes are 0.044 m (comprising 0.0288 m of settlement and 0.0154 m of heaving), 0.118 m (comprising 0.056 m of settlement and

0.0623 m of heaving) and 0.122 m (comprising 0.0593 m of settlement and 0.0636 m of heaving), respectively, for 2, 10 and 20 vehicle passes.

As mentioned in Section 3, the constitutive behaviour of elastic-perfectly plastic M-C model is capable in addressing the accumulative settlement provided that the yielding occurs at every stage of loading and reloading. For soil elements present in the uppermost levels of the model (having smaller depths from the loading boundary), the confining stresses are small, and hence the yield limits are also on the lower side. As the depth increases, the yield limits would increase with the increase in the confining pressures. Hence, at the lower depths, it is quite customary that each cycle of loading-unloading would lead to gradual accumulation of vertical displacement, with each unloading cycle having some partial elastic recovery. The amount of settlement and accumulation would gradually decrease with depth, and beyond a depth when the yield limit would not be exceeded, the settlements would be purely elastic and no such accumulation would be noticed. This occurs at quite a considerable depth below the surface and is not of importance for the present study. In the present study, all the deformations are measured at the aggregate surface, hence, the accumulation at every loading-unloading-reloading cycles can be observed, which is in corroboration to surface rutting phenomenon in roadways. Thus to observe the gradual accumulation of the permanent vertical displacement at every loading-unloading-reloading cycles, a node is slected at the center of the equivalent rectangular wheel load contact area, as shown by Point A in Fig. 15a. Figure 16 shows the vertical displacement at Point A against the dynamic time for 10 vehicular passes throught he unreinforced unpaved road. Following the loading pattern described in Fig. 8, it is observed that the peak discplacement at each vehicular pass is getting repeated at an interval 2 sec, thereby exhibiting proper application of repetitve vehicular load input. As the vehicle departs the section, an elastic rebound is noted over a small interval of time until it emerges into a final residual or permanent displacement, i.e. rutting. The elastic rebound occurs for around 1.2 s after the passage of the vehicular axle load. From the obervations, it can be understood that with each of the passes, there is an accumualtion of rutting at the surface of unpaved road. After 10 vehicle passes, the permanent vertical displacement is around 140 mm, which is nearly 2 times of the required serviceability criteria of 75 mm [22, 23, 51, 69].

5.2.2 Outcomes from a typical FE-based simulation for reinforced unpaved road under repetitive loading

It is understood from the previous section that with the increase in number of vehicular passes, the amount of rut also increases. Rutting not only damages the long-term performance of unpaved road, thereby increasing the regular maintenance cost, it also restricts the day-to-day comfort of commuters depending on the service of the road. In this regard, to seek out a sustainable alternative, a geotextile layer is introduced at the interface of aggregate and subgrade to reduce the rutting developed in unpaved road owing to repetitive vehicular loading. The response of unpaved road under repetitive vehicular load is checked for two different tensile modulus of the geotextile, i.e. 400 kN/m and 600 kN/m, respectively. The parametric properties of the model are kept same as that of the unreinforced case (as illustrated in Section 5.2.1).

Figure 17 shows the comparison of rutting developed between unreinforced and reinforced unpaved road due to 10 vehicle passes. It is to be noted that the rutting magnitudes shown in Fig. 17 are in exaggerated scale for intra-comparison and is not at the same scale of aggregate layer thickness. Similar comparative qualitative trend of

displacements of unreinforced and reinforced unpaved roads was also highlighted by Wu *et al.* [40] as well as Ingle and Bhosale [33]. In the present case, for a geotextile with tensile modulus 400 kN/m, maximum heaving and maximum settlement are obtained to be 0.037 m and 0.006 m respectively (adding to a rutting of 0.043 m), thereby reducing rut by 63% in comparison to unreinforced case. Similarly, for a geotextile with tensile modulus of 600 kN/m, maximum heaving and maximum settlement are 0.018 m and 0.006 m respectively (adding to a rutting of 0.024 m), thereby reducing the rutting approximately by 79% in comparison to unreinforced case. Leonardi et al. [7] exhibited a surface displacement reduction of 25% by the application of geogrid reinforcements in paved roads. In comparison to unreinforced unpaved road sections subjected to repeated loading, based on both laboratory and controlled field tests, researchers [20, 35] have highlighted an approximate reduction in surface displacement of about 50% when different types of geosynthetics, having varying tensile moduli, were used as reinforcement at the aggregate-subgrade interface. Based on moving wheel load tests, Singh *et al*. [18] highlighted a 30-40% improvement in surface displacements when geosynthetics of varying tensile strengths are used at the interface of aggregate and lime-stabilized subgrade. In a similar manner, Wu et al. [40] exhibited an improvement of 40-70% when geogrids of various tensile modulus are used to reinforce the unpaved section by their placement at the aggregate-subgrade interface. Thus, it is understood that with increase in the axial stiffness of the geotextile reinforcement, the overall rutting of the unpaved road system reduces significantly, thereby increasing the service life of the system. Hence, placement of geotextile reinforcement can be considered a sustainable solution for enhancing the longevity of unpaved roads.

Figure 18 shows the vertical displacement against the dynamic time averaged over the section B-B connecting the edges of the wheel load (as shown in Fig. 15a). Similar to the former observation, it is observed that for unreinforced case, there is a recognizable increase in permanent vertical displacement after each vehicular cycle for a total of 10 passes. However, it is to be noted that the displacement at the centre of the wheel (as in Fig. 16) is evidently more than that observed in the edges of the wheel (as in Fig. 18). It is worth mentioning that the magnitude of permanent displacement attained after 10 cycles in this numerical simulation, i.e. around 85 mm, conforms to a similar magnitude reported by Perkins *et al*. [37] from similar experimental investigations. Figure 18 also exhibits the observed vertical displacement for 10 vehicle passes when a layer of geotextile of varying axial stiffness, i.e. 400 kN/m and 600 kN/m, is applied at the aggregate-subgrade interface. It is observed that inclusion of geotextile reinforcement aided in substantial reduction in the vertical displacement at the surface of the unpaved road, thereby elucidating the successful reinforcing action of geosynthetic. For reinforced unpaved road, the permanent vertical displacement after 10 cycles are approximately noted to be 7 mm and 6 mm when geotextile with tensile modulus 400 kN/m and 600 kN/m, respectively, is used. Similarly, based on controlled field tests, significant reduction in rut depth was also reported by Latha *et al*. [35] when different types of geosynthetics having varying tensile moduli was used as reinforcement at the aggregate-subgrade interface. It is worth mentioning that the vertical deformation keeps on marginally decreasing with the increase in number of vehicle passes in reinforced case owing to the tension membrane effect rendered by the stretched geotextile. In this process, the rutting (summation of maximum displacement and maximum heaving) attains a nearly constant magnitude, thereby enhancing the sustainability of the reinforced unpaved road system.

Figure 17 and 18 comprehensibly delineates the beneficial and sustainable application of geotextile in arresting the permanent vertical displacement beneath the wheels as well as rutting in unpaved road system. Geotextiles, with properly chosen axial stiffness, not only substantially reduces the rutting in comparison to the unreinforced unpaved roads, it is also largely successful in arresting the rutting and preventing the accumulation of rutting under higher number of vehicular load cycles. This transcribes to the understanding that properly chosen geotextile and their proper implementation in the construction practices of unpaved roads can significantly enhance the performance and sustainability of the same.

6. Conclusions and Recommendations

This paper illustrates the necessity of using geotextile as reinforcement in design of unpaved road resting on marginalized soil with the aid of a coupled stress-deformation based approach. In the earlier proposed design methods, the thickness of aggregate layer in unpaved road was determined based on conventional two-dimensional limit equilibrium approach considering plane strain equilibrium of the stresses from applied strip loading representing the wheel to the undrained bearing capacity of soft cohesive soils. In the present study, the limit equilibrium-based approach is processed with the three-dimensional load-dispersion of stresses through aggregate layer is considered and a modified expression for assessing the aggregate layer thickness is proposed considering the shape of the equivalent contact area of a dual wheel system. Conventional limit equilibrium-based approach considers the individual component of unpaved road to be non-deformable, thereby eventually leading to a conservative design. Therefore, a stress-deformation approach based design is considered in this study to simulate FE models of the real field behaviour of unpaved roads under vehicular loads. The paper illustrated the results for both unreinforced and geotextile reinforced unpaved road under quasi-static and repetitive loading conditions. The benefits of using geosynthetic in overall stability of the unpaved road under different operational conditions is administered. Following are the list of important outcomes and conclusions from the present study:

- A FE-based step-by-step design methodology of unpaved road resting on marginalized soil subgrade under quasi-static and repetitive loading conditions is proposed while incorporating different operational conditions that are not considered in conventional limit equilibrium based design. Through the FE-based design, the necessity of improvement in strength of the individual component of the unpaved road is illustrated so that the operational failures can be suitably averted.
- Introduction and application of geotextiles at the aggregate-subgrade interface leads to substantial improvement of the unpaved road system over its unreinforced state. For unpaved roads resting on marginalized soil subgrade, inclusion of geotextile having with axial stiffness 400 kN/m or higher is enough to counteract the stresses coming from aggregate loading and prevent the corresponding operational failure. With the choice of geotextile with even higher tensile modulus, there is further decrease in the strain accumulation in the soil subgrade layer occurs and for a geotextile with tensile modulus greater 1000 kN/m, the strain accumulation becomes negligible.
- FE models developed for unpaved road built on marginalized soil subgrade successfully depicted the rutting behavior and accumulation of permanent vertical displacement under increasing number of repetitive vehicular loading. For a typical unreinforced unpaved road, accumulated vertical displacement was found to surpass the limiting serviceability criterion for rutting after 10 vehicular passes. This would

render the unreinforced unpaved road unusable in the long run and would require ground improvement or strengthening by geotextile reinforcement.

- The surface rutting in an unpaved road is significantly reduced by incorporating a geotextile layer at the interface of the aggregate and subgrade. The tensile modulus of geotextile governs the reduction in rutting in comparison to unreinforced scenarios. For a typical unpaved road system, a geotextile with higher axial stiffness, such as 400-600 kN/m, is capable of reducing the rutting by almost 63-79% to that obtained for an unreinforced scenario. Presence of geotextile also arrests the vertical displacement beneath the wheels under repeated loading owing to the tension membrane effect imparted by their progressively stretched form.

With rapid industrialization, the global natural reserve of good quality raw material for construction of road network is depleting. Added to that, the use of poor quality of locally available marginal materials as aggregates also hampers the long-term performance of unpaved roads that starts exhibiting significant and uncontrollable rutting. Conventionally adopted ground improvement proves to be costly when it is adopted for long stretches of road network. In this regard, use of geosynthetic proves to be sustainable solution offering durability and long-term performance of the unpaved road by controlling the rutting within serviceability criteria and not allowing the rutting to progressively accumulate with increasing number of vehicles passes.

Funding Statement

This research did not receive any specific grant from funding agencies like public, commercial or non-profit sectors.

Data Availability Statement

Data sets generated during the current study are available from the corresponding author on reasonable request.

Conflict of Interest

The authors declare that they have no conflict of interest.

References

1. Faiz AJ (2012) The promise of rural roads: Review of the role of low-volume roads in rural connectivity, poverty reduction, crisis management, and livability. Transportation Research Circular E-C167, Transportation Research Board, Washington, DC, USA. https://onlinepubs.trb.org/onlinepubs/circulars/ec167.pdf
2. MORTH (2021) Road transport year book 2017-18 and 2018-19. Transport Research Wing, Ministry of Road Transport and Highways, New Delhi, India. https://morth.nic.in/sites/default/files/RTYB-2017-18-2018-19.pdf
3. CIA (2023) The world fact book, field listings – Roadways. https://www.cia.gov/the-world-factbook/countries/united-states. Accessed 6th June 2023.
4. Skorseth K, Reid R and Heiberger K (2015) Gravel Roads: Construction and Maintenance Guide. US Department of Transportation, Federal Highway Administration, Washington DC, USA. https://www.fhwa.dot.gov/construction/pubs/ots15002.pdf

5. Paige-Green P, Pinard M, Netterberg F (2015) A review of specifications for lateritic materials for low volume roads. Transp Geotech 5:86-98. http://dx.doi.org/10.1016/j.trgeo.2015.10.002
6. Mendoza A, Guaje J, Enciso C, Beltran G (2022) Mechanical behavior assessment of tire-reinforced recycled aggregates for low traffic road construction. Transp Geotech 33:1-8. https://doi.org/10.1016/j.trgeo.2022.100730
7. Leonardi G, Bosco DL, Palamara R, Suarci F (2020) Finite element analysis of geogrid-stabilized unpaved roads. Sustainability 12(5):1-11. https://doi.org/10.3390/su12051929
8. Gourley, CS (1997) Lightly trafficked sealed roads in southern Africa: Flexibility in design and construction. First International Symposium on Paving of Low Volume Roads, Rio de Janeiro, Brazil, pp. 745-762. https://citeseerx.ist.psu.edu/document?repid=rep1&type=pdf&doi=d0eca2f9ec2b16759931cbb9cd142d600d3d5f89
9. Shoop S, Haehnel R, Janoo V, Harjes D, Liston R (2006) Seasonal deterioration of unsurfaced roads. J Geotech Geoenviron Eng ASCE 132(7):852-860. https://doi.org/10.1061/(ASCE)1090-0241(2006)132:7(852)
10. Jones D, Paige-Green P (2015) Limitations of using conventional unpaved road specifications for understanding unpaved road performance. Transp Res Rec 2474(1):30-38. https://doi.org/10.3141/2474-04
11. Le Vern M, Razamkamantsoa A, Murzyn F, Larrarte F, Cerezo V (2022) Effects of soil surface degradation and vehicle momentum on dust emissions and visibility reduction from unpaved roads. Transp Geotech 37:1-12. https://doi.org/10.1016/j.trgeo.2022.100842
12. Ibagon L, Caicedo B, Villaceres JP, Yepez F (2023) Modelling of washboard effect on unpaved roads experimental evidence on non-cohesive materials. Transp Geotech 41:101015. https://doi.org/10.1016/j.trgeo.2023.101015
13. Fannin RJ, Sigurdsson O (1996) Field observations on stabilization of unpaved roads with geosynthetics. J Geotech Eng ASCE 122(7):544-553. https://ascelibrary.org/doi/10.1061/%28ASCE%290733-9410%281996%29122%3A7%28544%29
14. Calvarano LS, Palamara R, Leonardi G, Moraci N (2016) Unpaved road reinforced with geosynthetics. Proce Eng 158:296-301. https://doi.org/10.1016/j.proeng.2016.08.445
15. Buonsanti M, Leonardi G, Scopelliti F (2012) Theoretical and computational analysis of airport flexible pavements reinforced with geogrids. In: Proceeding 7th RILEM International Conference on Cracking in Pavements, Vol. 4, pp 1219–1227. https://doi.org/10.1007/978-94-007-4566-7_116
16. Calvarano LS, Leonardi G, Palamar R (2017) Finite element modelling of unpaved road reinforced with geosynthetics. Proce Eng 189:99 –104. https://doi.org/10.1016/j.proeng.2017.05.017
17. Vaitkus A, Siukscius A, Ramūnas V (2014) Regulations for use of geosynthetics for road embankments and subgrades. Baltic J Road Bridge Eng 9(2):88–93. https://bjrbe-journals.rtu.lv/article/view/bjrbe.2014.11
18. Singh M, Trivedi A, Shukla SK (2022) Evaluation of geosynthetic reinforcement in unpaved road using moving wheel load test. Geotex Geomem 50(4):581–589. https://doi.org/10.1016/j.geotexmem.2022.02.005

19. Alkaissi ZA, Al-Soud, MS (2021) Effect of geogrid reinforcement on behavior of unpaved roads. IOP Conf Ser: Earth Env Sc 856: 012007-1-8. http://dx.doi.org/10.1088/1755-1315/856/1/012007
20. Nair AM, Latha GM (2016) Repeated load tests on geosynthetic reinforced unpaved road sections. Geomech Geoengg 11(2): 95-103. http://dx.doi.org/10.1080/17486025.2015.1029012
21. Singh M, Trivedi A, Shukla SK (2020) Influence of geosynthetic reinforcement on unpaved roads based on CBR, and static and dynamic cone penetration tests. Int J Geosyn Gr Eng 6:1-13. https://doi.org/10.1007/s40891-020-00196-0
22. Giroud J, Noiray L (1981) Geotextile-reinforced unpaved road design. J Geotech Eng Div ASCE 107(9):1233-1254. https://ascelibrary.org/doi/10.1061/AJGEB6.0001187
23. Holtz R, Sivakugan N (1987) Design charts for roads with geotextiles. Geotext Geomembranes 5(3):191-199. https://www.sciencedirect.com/science/article/abs/pii/0266114487900161
24. Bourdeau PL, Holtz RD, Chapuis J (1988) Effect of anchorage and modulus in geotextile-reinforced unpaved roads. Geotex Geomem 7(3):221-30. https://doi.org/10.1016/0266-1144(88)90010-6
25. Douglas RA, Kelly MA (1986) Geotextile reinforced unpaved logging roads: The effect of anchorage. Geotex Geomem 4(2):93-106. https://doi.org/10.1016/0266-1144(86)90018-X
26. Milligan G, Jewell R, Houlsby G, Burd H (1989) A new approach to the design of unpaved roads – Part I. Ground Eng 22(3):25-29. https://cdn.ca.emap.com/wp-content/uploads/sites/13/1989/04/1989-04_Pages_25-29.pdf
27. Milligan G, Jewell R, Houlsby G, Burd H (1989) A new approach to the design of unpaved roads – Part II. Ground Eng 23(8):37-42. https://cdn.ca.emap.com/wp-content/uploads/sites/13/1989/11/1989-11_Pages_37-42.pdf
28. Tingle JS, Webster SL (2003) Review of corps of engineers' design of geosynthetic-reinforced unpaved roads. Transp Res Rec 1849:193-201. https://doi.org/10.3141/1849-21
29. Army and Air Force (1995) Engineering use of geotextiles. Army Technical Manual TM 5-818-8 (Air Force Joint Manual AFJMAN 32-1030). Headquarters, U.S. Departments of the Army and Air Force, Washington DC, USA. https://www.wbdg.org/FFC/ARMYCOE/COETM/ARCHIVES/tm_5_818_8.pdf
30. Giroud JP, Han J (2004a) Design methods for geogrid-reinforced unpaved roads I-Development of design method. J Geotech Geoenviron Eng ASCE 130(8):775-786. https://doi.org/10.1061/(ASCE)1090-0241(2004)130:8(775)
31. Giroud JP, Han J (2004b) Design methods for geogrid-reinforced unpaved roads II-Calibration and application. J Geotech Geoenviron Eng ASCE 130(8):787-797. https://doi.org/10.1061/(ASCE)1090-0241(2004)130:8(787)
32. Tingle JS, Jersey SR (2005) Cyclic plate load testing of geosynthetic-reinforced unbound aggregate roads. Transp Res Rec: J Transp Res B 1936: 60-69. https://doi.org/10.1177/0361198105193600108
33. Hufenus R, Rueegger R, Banjac R, Mayor P, Springman SM, Bronnimann R (2006) Full-scale field tests on geosynthetic reinforced unpaved roads on soft subgrade. Geotext Geomembranes 24(1):21–37. https://doi:10.1016/j.geotexmem.2005.06.002
34. Lyons CK, Fannin J (2006) A comparison of two design methods for unpaved roads reinforced with geogrids. Can Geotech J 43:1389-1394. https://cdnsciencepub.com/doi/10.1139/t06-075

35. Latha GM, Nair AM, Hemalatha MS (2010) Performance of geosynthetics in unpaved roads. Int J Geotech Eng 4:337-349. http://dx.doi.org/10.3328/IJGE.2010.04.02.337-349
36. Mekkawy MM, White DJ, Suleiman MT, Jahren CT (2011) Mechanically reinforced granular shoulders on soft subgrade: Laboratory and full-scale studies. Geotex Geomem 29 (2011):149-160. http://dx.doi.org/10.1016/j.geotexmem.2010.10.006
37. Perkins SW, Christopher BR, Lacina BA, Klompmaker J (2012) Mechanistic-empirical modeling of geosynthetic-reinforced unpaved roads. Int J Geomech, ASCE 12(4):370-380. http://dx.doi.org/10.1061/(ASCE)GM.1943-5622.0000184
38. Yang X, Han J, Pokharel SK, Manandhar C, Parsons RL, Leshchinsky D, Halahmi I (2012) Accelerated pavement testing of unpaved roads with geocell-reinforced sand bases. Geotex Geomem 32 (2012):95-103. http://dx.doi.org/10.1016/j.geotexmem.2011.10.004
39. Ravi K, Dash SK, Vogt S (2014) Behaviour of geosynthetic reinforced unpaved roads under cyclic loading. Ind Geotech J 44(1):77–85. http://dx.doi.org/10.1007/s40098-013-0051-9
40. Wu H, Huang B, Shu X, Zhao S (2015) Evaluation of geogrid reinforcement effects on unbound granular pavement base courses using loaded wheel tester. Geotex Geomem 43 (2015):462-469. http://dx.doi.org/10.1016/j.geotexmem.2015.04.014
41. Suku L, Prabhu SS, Ramesh P, Babu GLS (2016) Behavior of geocell-reinforced granular base under repeated loading. Transp Geotech 9:17–30. http://dx.doi.org/10.1016/j.trgeo.2016.06.002
42. Ingle GS, Bhosale SS (2017) Full-scale laboratory accelerated test on geotextile reinforced unpaved road. Int J Geosyn Gr Eng 3:33. http://dx.doi.org/10.1007/s40891-017-0110-x
43. Demir A, Sarici T, Ok B, Demir B, Komut M, Comez S, Mert A (2018) Large scale tests for geogrid reinforced unpaved roads. Proc. 11th Int Conf Geosynth, Seoul, South Korea, 1-8. https://library.geosyntheticssociety.org/wp-content/uploads/resources/proceedings/122021/S19-04.pdf
44. Singh M, Trivedi A, Shukla SK (2019) Strength enhancement of the subgrade soil of unpaved road with geosynthetic reinforcement layers Transp Geotech 19:54–60. https://doi.org/10.1016/j.trgeo.2019.01.007
45. Han B, Ling J, Shu X, Song W, Boudreau RL, Hu W, Huang B (2019) Quantifying the effects of geogrid reinforcement in unbound granular base. Geotex Geomem 47(3):369–376. https://doi.org/10.1016/j.geotexmem.2019.01.009
46. Khoueiry N, Briançon L, Riot M, Daouadji A (2021) Full-scale laboratory tests of geosynthetic reinforced unpaved roads on a soft subgrade. Geosyn Int 28(4):435-449. https://doi.org/10.1680/jgein.21.00001
47. Biswas S, Hussain M, Singh KL (2024) Behavior of bamboo and jute geocell overlaying soft subgrade under repeated wheel loading. J Mater Civ Eng 36(2): 04023570-1-12. https://doi.org/10.1061/JMCEE7.MTENG-16528
48. Maxwell S, Kim W-H, Edil TB, Benson CH (2015) Effectiveness of geosynthetics in stabilizing soft subgrades. Wisconsin Highway Research Program Report 0092-45-15, Wisconsin Department of Transportation, Madosin, USA. https://wisconsindot.gov/documents2/research/45-15geosyn1.pdf
49. Kumar S, Singh SK (2023) Subgrade soil stabilization using geosynthetics: A critical review. Mat Today Proc, Article in Press, 1-5. https://doi.org/10.1016/j.matpr.2023.04.266

50. Meena S, Choudhary L, Dey A (2013) Quasi-static analysis of geotextile-reinforced unpaved road resting on *c-φ* subgrade. Proce- Soc Behav Sci 104:235–244. https://doi.org/10.1016/j.sbspro.2013.11.116
51. Sarma NJ, Dey A (2024) Finite element-based design and analysis of unpaved roads over difficult subsoil: Sustainable application of geotextile reinforcement to attain long-term performance. Indian Geotech J 1-28. https://doi.org/10.1007/s40098-024-00866-0
52. Vern ML, Doré G, Bilodeau JP (2016) Mechanistic-empirical design of unpaved roads. In: TAC 2016-Efficient Transportation-Managing the Demand, 2016 Conference of the Transportation Association, Toronto, Canad, 1-19. https://www.tac-atc.ca/sites/default/files/conf_papers/levern.pdf
53. Zarnani S, Bathurst RJ (2008) Numerical modeling of EPS seismic buffer shaking table tests. Geotex Geomem 26:371-383. https://doi.org/10.1016/j.geotexmem.2008.02.004
54. Labuz JF, Zhang A (2012) Mohr-Coulomb failure criterion. Rock Mech Rock Eng 45:975-979. https://doi.org/10.1007/s00603-012-0281-7
55. Cui XZ, Jin Q, Shang QS, Liu ST (2006) Mohr-Coulomb model considering variation of elastic modulus and its application. Key Eng Mat 306-388:1445-1448. https://doi.org/10.4028/www.scientific.net/KEM.306-308.1445
56. Zarnani S, Bathurst RJ (2009) Influence of constitutive model on numerical simulation of EPS seismic buffer shaking table tests. Geotex Geomem 27:308-312. https://doi.org/10.1016/j.geotexmem.2008.11.008
57. Zarnani S, El-Emam MM, Bathurst RJ (2011) Comparison of numerical and analytical solutions for reinforced soil wall shaking table tests. Geomech Eng 3(4):291-321. https://doi.org/10.12989/gae.2011.3.4.291
58. Lade PV (2005) Overview of constitutive models for soils. In: Geotechnical Special Publications No. 128, pp 1-34. https://doi.org/10.1061/40771(169)1
59. Yaghoubi E, Arulrajah A, Wong Y, Horpibulsuk S (2016) Stiffness properties of recycled concrete aggregate with polyethylene plastic granules in unbound pavement applications. J Mat Civil Eng ASCE 29(4):04016271-1-7. https://doi.org/10.1061/(ASCE)MT.1943-5533.0001821
60. MORTH (2000) Specification of maximum gross vehicle weight and maximum safe axle weight. Notification by Transport Wing, Ministry of Road Transport and Highways, Government of India.
61. https://www.easternplanthire.com/2020/01/10/the-worlds-top-5-biggest-mining-dump-trucks-2020 (Last Accessed: 17.03.2024)
62. Roy SS, Deb K (2019) Interference effect of closely spaced footings resting on granular fill over soft clay. Int J Geomech ASCE 19(1):04018181-1-17.
63. Terzaghi K (1943) Theoretical Soil Mechanics. John Wiley and Sons, New York, USA.
64. Shen S, Carpenter SH (2007) Dissipated energy concepts for HMA performance: Fatigue and healing. COE Rep No. 29, Adv Transp Res Eng Lab (ATREL), University of Illinois-Urbana Champaign, USA. https://hdl.handle.net/2142/83306
65. Tao M and Abu-Farsakh MY (2008) Effect of Drainage in Unbound Aggregate Bases on Flexible Pavement Performance. Rep No. FHWA/LA.07/429, Lousiana Transp Res Center, Baton Rouge, Lousiana, USA. https://rosap.ntl.bts.gov/view/dot/22123

66. Abu-Farsakh MY, Chen Q (2011) Evaluation of geogrid base reinforcement in flexible pavement using cyclic plate load testing. Int J Pav Eng. 12:275–288. https://doi.org/10.1080/10298436.2010.549565
67. Kirsch K, Bell A (2013) Ground Improvement. CRC Press, Boca Raton, USA.
68. Chattopadhyay BC, Maity J (2017) Ground Improvement Techniques. PHI, New Delhi, India.
69. ASTM E1703/E1703M-10 (2015) Standard test method for measuring rut-depth of pavement surfaces using a straightedge. ASTM International, West Conshohoken, PA, USA. https://www.astm.org/e1703_e1703m-10r15.html

Table 1 Stiffness properties of materials used in the FE simulations of unpaved roads in the present study

	Subgrade	**Aggregate**
Soil model	Mohr-Coulomb	Mohr-Coulomb
Unit weight (γ)	19 kN/m^3	19 kN/m^3
Elastic modulus (E)	20 MPa	60 MPa
Poisson's ratio (ν)	0.4	0.3

Table 2 Material properties used in the FE model developed for validation study

	Top sand layer	**Bottom soft clay**
Soil model	Mohr-Coulomb	Mohr-Coulomb
Unit weight (γ)	15.7 kN/m^3	17.17 kN/m^3
Elastic modulus (E)	1000 kPa	5000 kPa
Poisson's ratio (ν)	0.15	0.4
Cohesion (c)	0.5 kPa	7.2 kPa
Angle of Internal Friction (φ)	38^o	–

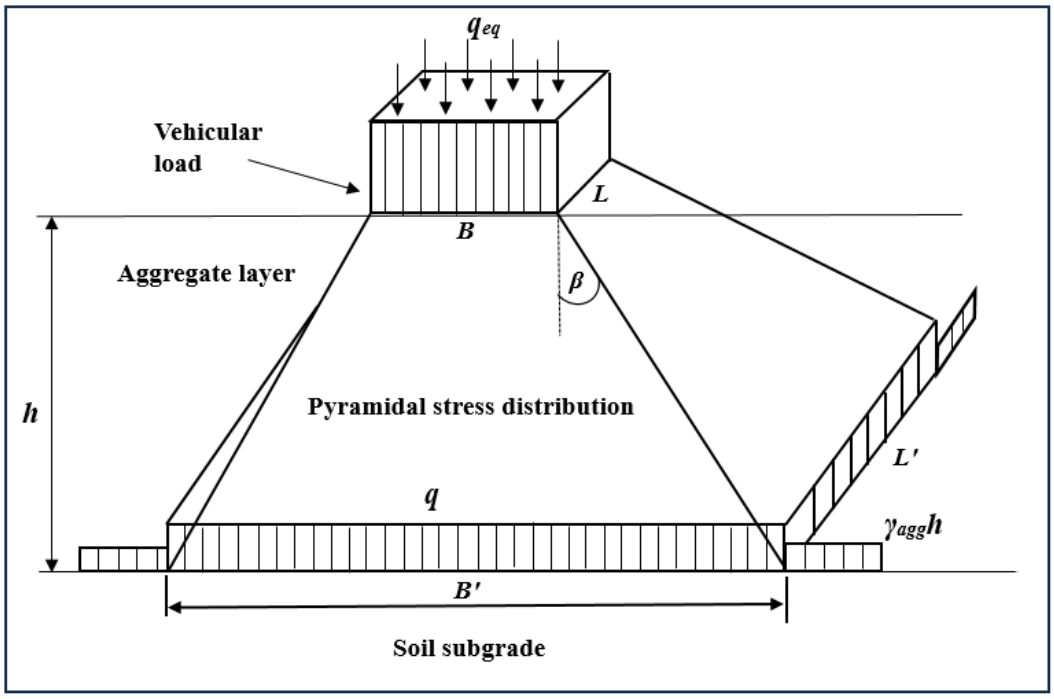

Fig. 1 3D pyramidal load distribution through the aggregate layer

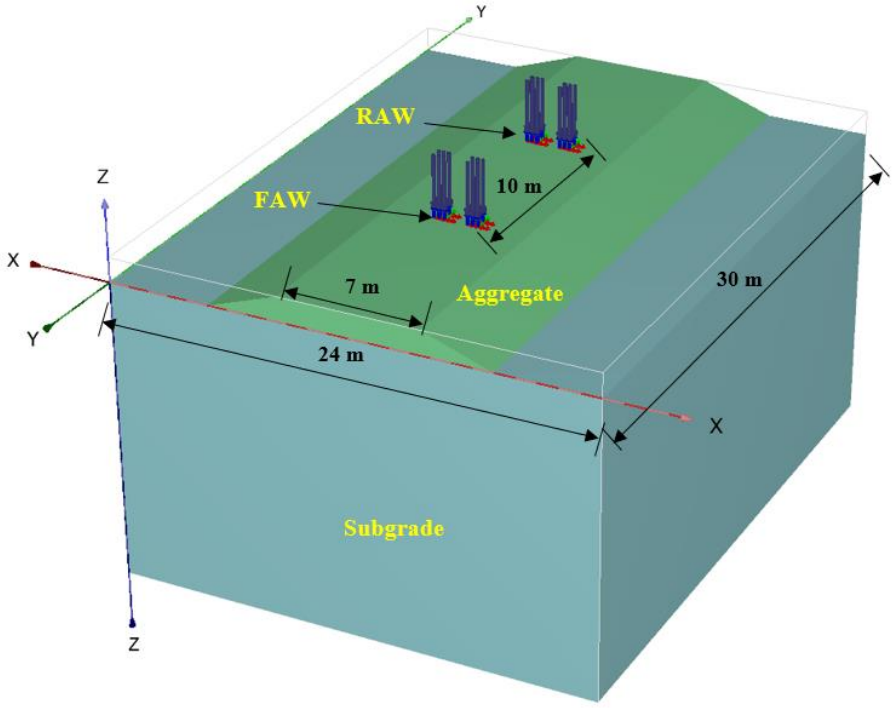

Fig. 2 Finite element model of unreinforced unpaved road in PLAXIS 3D

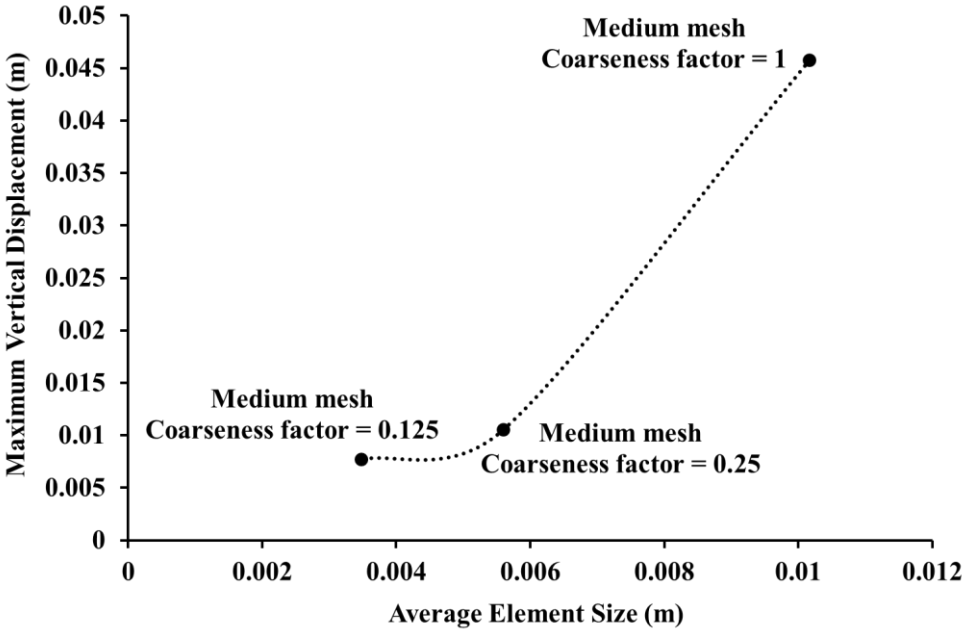

Fig. 3 Optimal mesh size determination from mesh convergence study

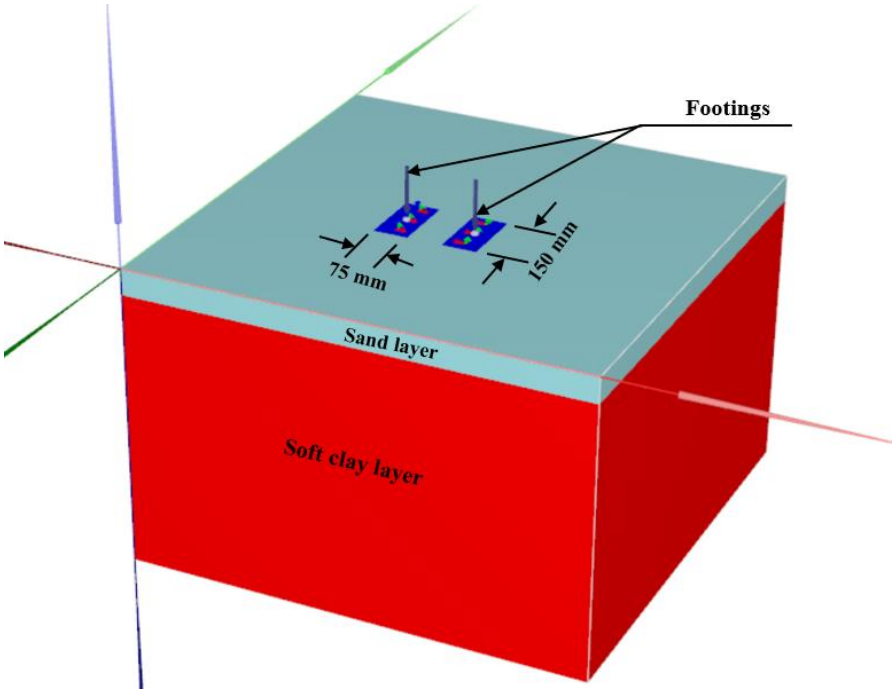

Fig. 4 FE model developed for the validation study following the experimental investigation by Roy and Deb [62]

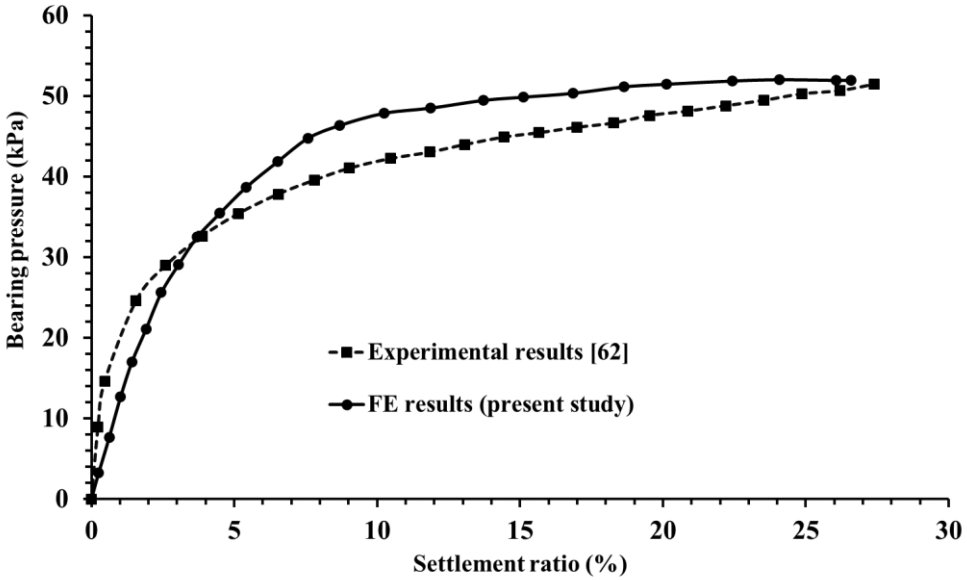

Fig. 5 Comparison of pressure-settlement plots from experimental investigation and FE model used for validation

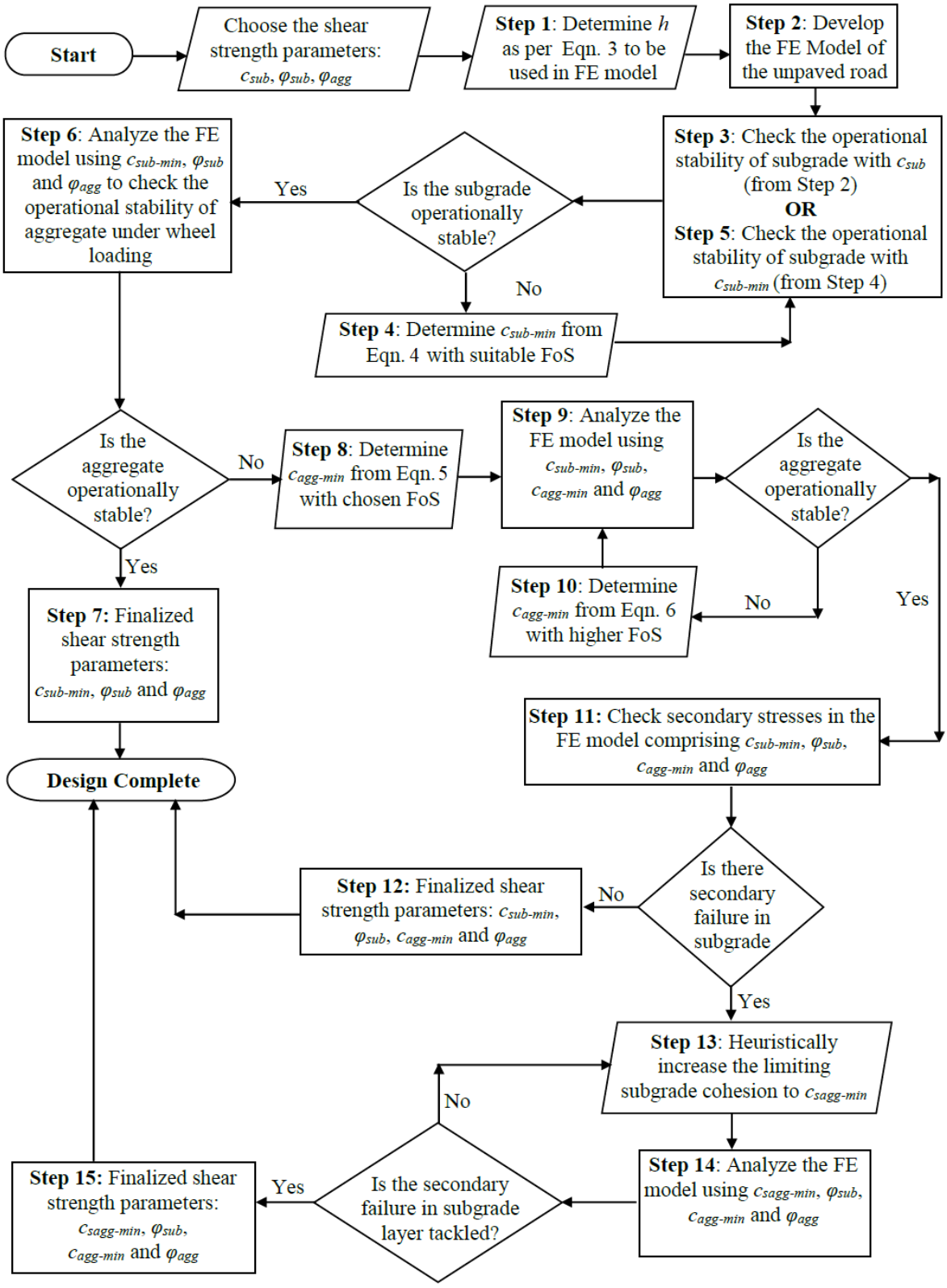

Fig. 6 Flowchart depicting the algorithmic step-by-step design of unreinforced unpaved road

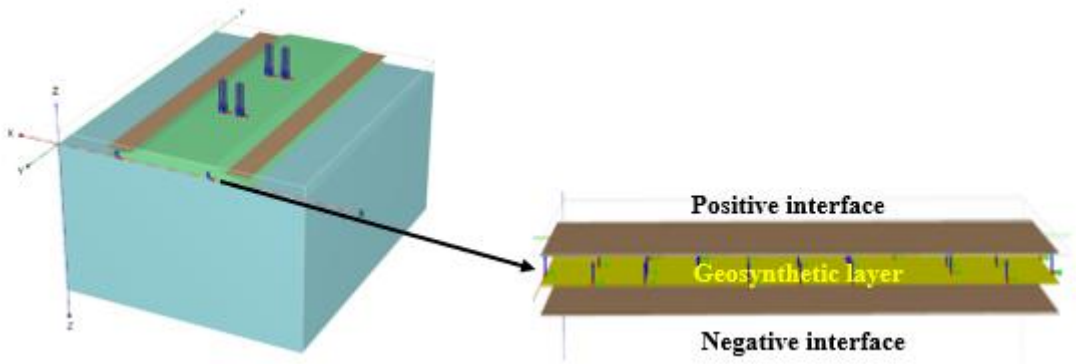

Fig. 7 FE model of reinforced unpaved road exhibiting geosynthetic and its interfaces

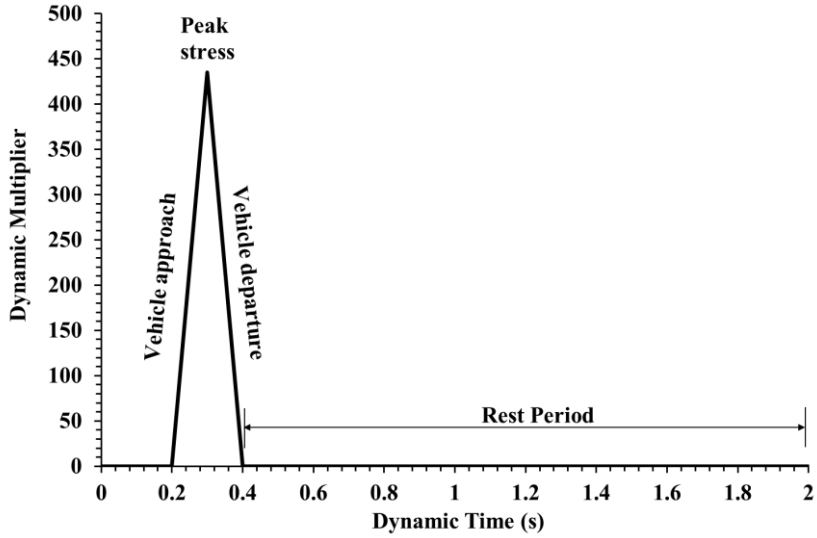

Fig. 8 Triangular load distribution signifying the quasi-dynamic multiplier for single vehicular passage

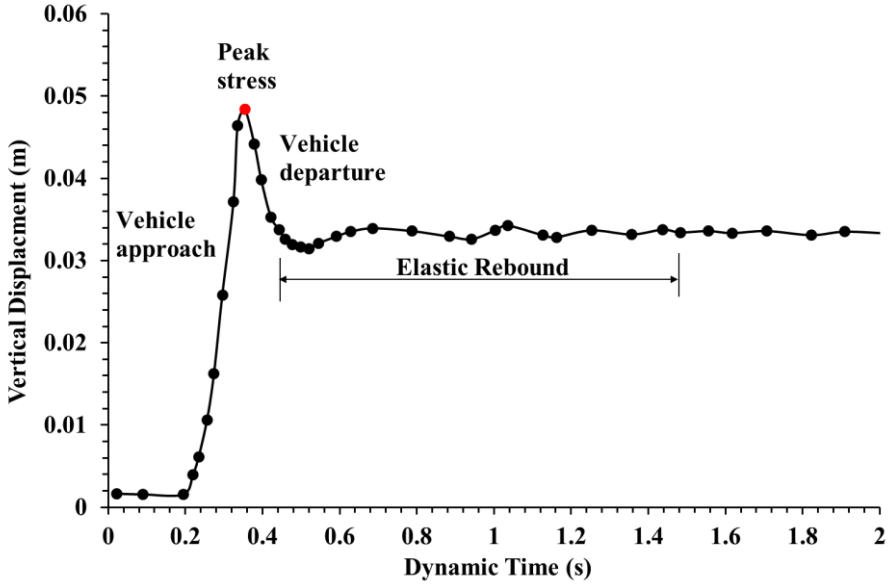

Fig. 9 Variation of vertical displacement beneath the wheel for a single passage of vehicle

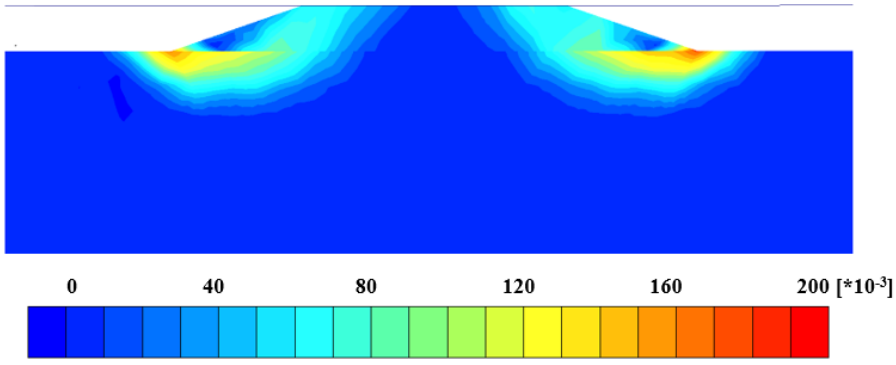

Fig. 10 Total deviatoric strain diagram of unpaved road subjected to aggerate loading on subgrade before improvement

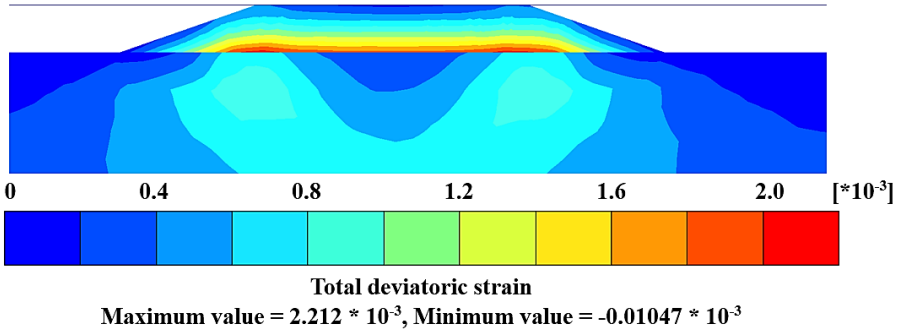

Fig. 11 Total deviatoric strain diagram of unpaved road subjected to aggregate load after improvement

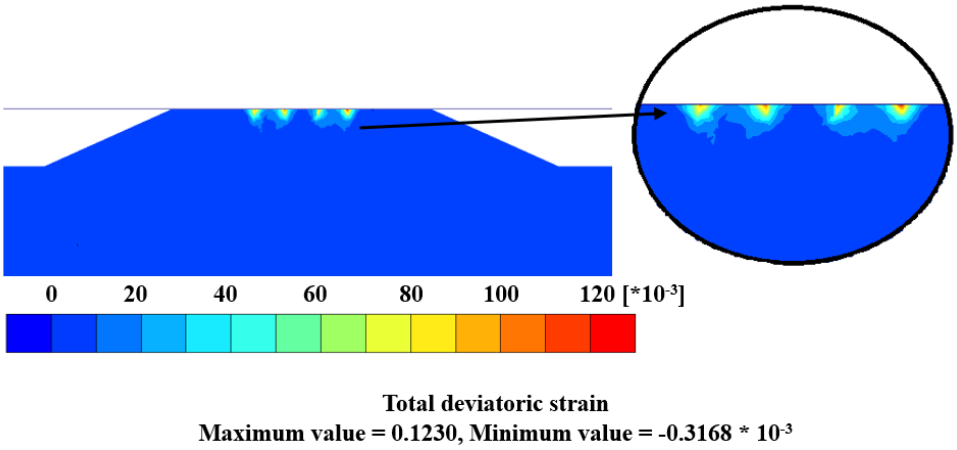

Fig. 12 Total deviatoric strain diagram of unpaved road subjected to vehicular load before improvement

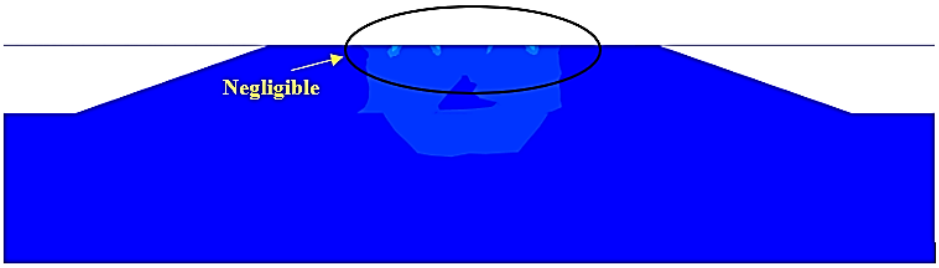

Fig. 13 Total deviatoric strain diagram of unpaved road subjected to vehicular load after improvement

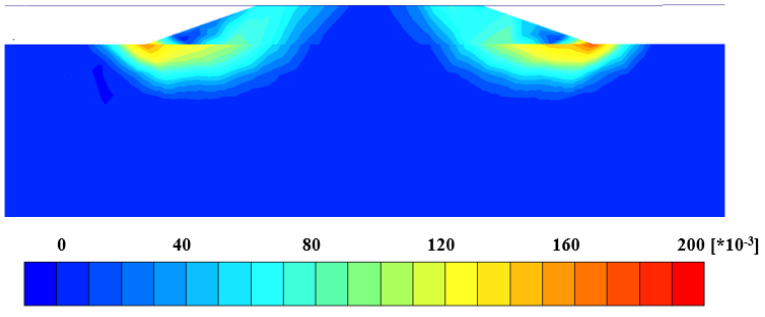

Total deviatoric strain
Maximum value = 0.1931, Minimum value = -0.7443 * 10^{-3}

(a)

Total deviatoric strain
Maximum value = 0.06912, Minimum value = 0.02536 *10^{-3}

(b)

Total deviatoric strain
Maximum value = 6.331*10^{-3}, Minimum value = 8.894 *10^{-6}

(c)

Fig. 14 FE model of unpaved road subjected to aggregate load (a) unreinforced condition and (b) reinforced condition (tensile modulus = 400 kN/m) (c) reinforced condition (tensile modulus = 1000 kN/m)

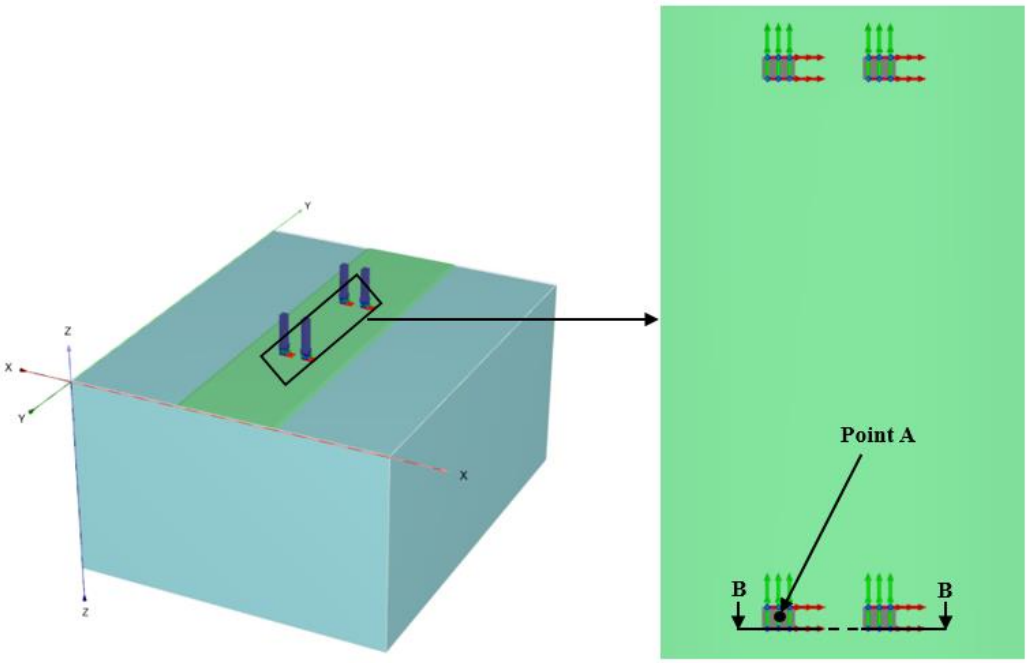

(a)

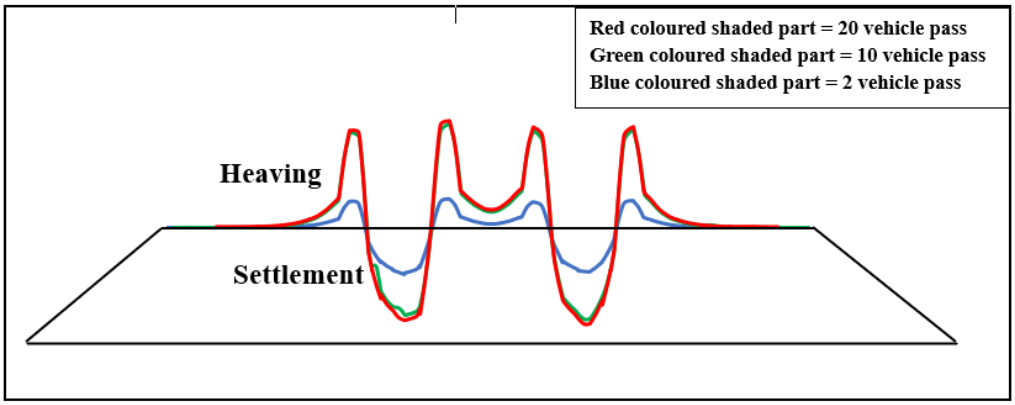

(b)

Fig. 15 Comparison of rutting developed in unreinforced unpaved road due to repetitive load from vehicular cycles comprising 2, 10 and 20 vehicle passes (NB: The rutting magnitudes are shown in exaggerated scale for intra-comparison and is not at the same scale of aggregate layer thickness)

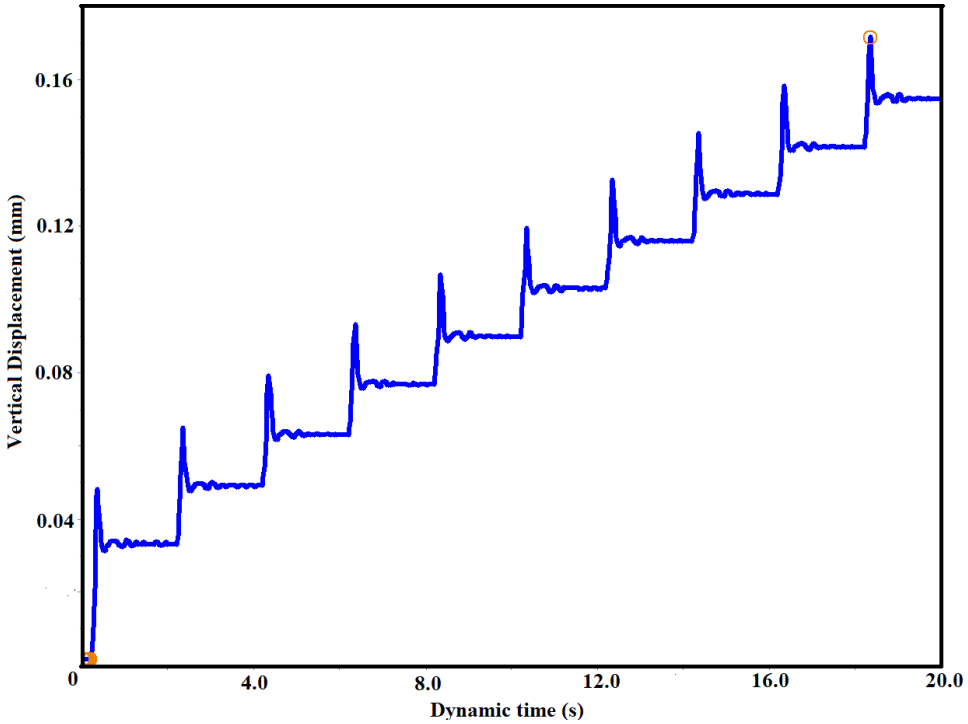

Fig. 16 Vertical displacement at Point A for 10 vehicular passes on unreinforced unpaved road

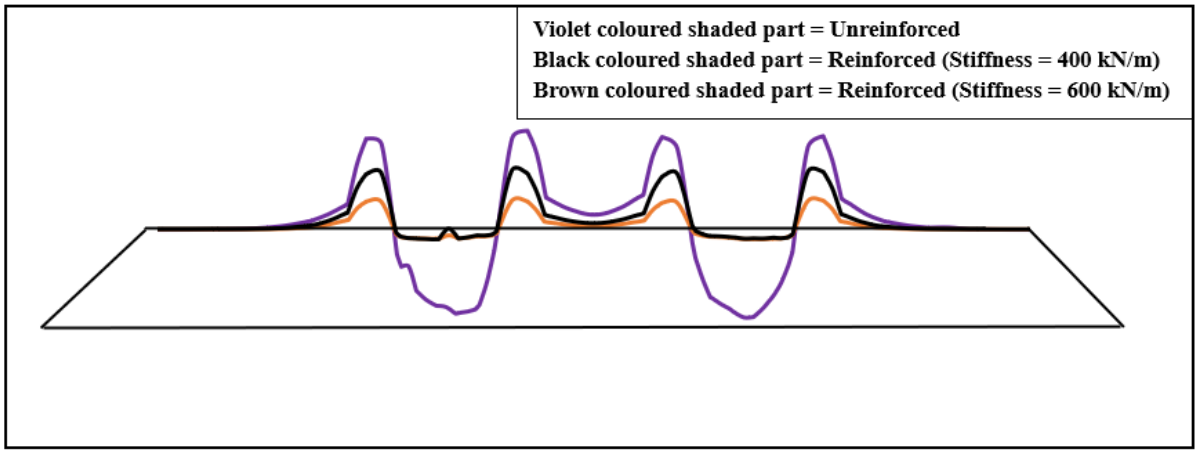

Fig. 17 Comparison of rutting developed between unreinforced and geotextile reinforced unpaved road due to repetitive vehicular load of 10 cycles (NB: The rutting magnitudes are shown in exaggerated scale for intra-comparison and is not at the same scale of aggregate layer thickness)

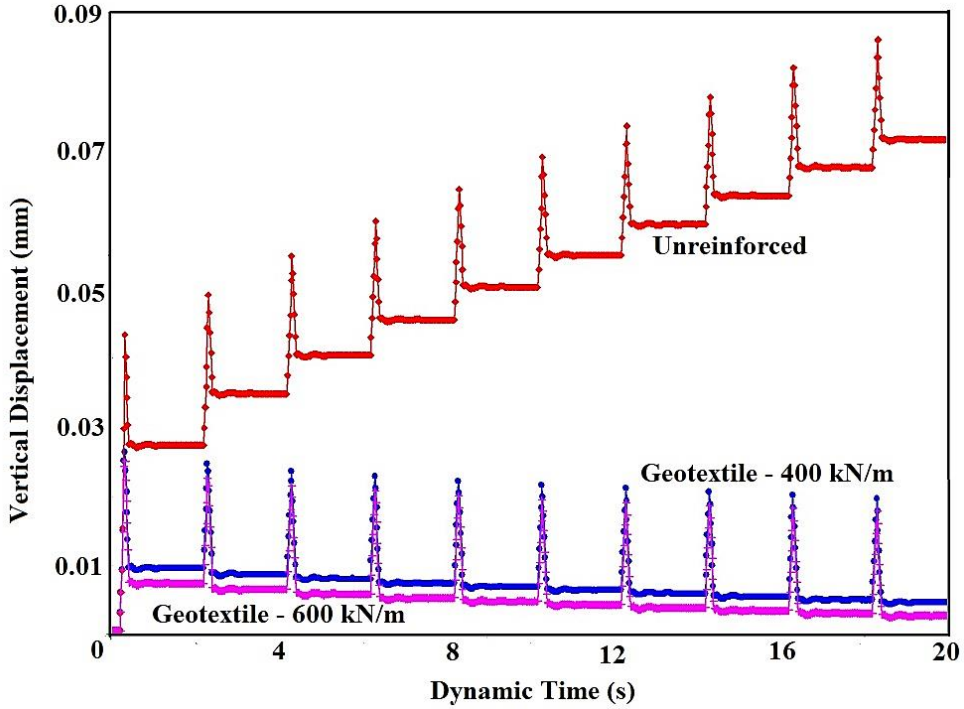

Fig. 18 Comparison of vertical displacement in the surface of unreinforced (Section B-B) and geotextile reinforced unpaved road after 10 vehicular passes using geotextiles of varying axial stiffness

Response to Reviewer Comments

Manuscript No.: **IGGE-D-23-00358**

Manuscript Title: **Improvement of Long-Term Performance of Unpaved Road constructed over marginalized Subsoil using Geotextile Reinforcement**

The authors whole-heartedly thank the reviewers for their thorough reading through the paper and providing numerous constructive comments that have been immensely helpful to improve upon the quality and clarity of the paper. The authors have responded on point-to-point basis on all the comments and queries raised by the esteemed reviewers. According to the suggestions, all the modifications have been made in the revised manuscript to the best of the authors' knowledge.

Response to Reviewer-1 Comments

Reviewer #1: The present study highlights a design methodology of unreinforced unpaved roads considering a coupled stress-deformation approach incorporating operational failure conditions under quasi-static loading conditions. Study shows that an additional geotextile layer at the aggregate-subgrade interface successfully reduces operational failure. Additionally, three-dimensional finite element analysis insights of reduction of rutting failure of pavement with the inclusion of geotextile layer. Study shows the sustainable use of geotextile in improving the performance of unpaved roads under repetitive loading.
However, the manuscript needs certain corrections before publishing in the journal.

Comment 1: How does the author derive the final equation (1)? Please describe it in detail.
Response: In the revised manuscript, details on derivation of Equation 1 is provided. In order to include some other equations in the derivation, Equation 1 is renumbered as Equation 3 in the revised manuscript.

Comment 2: In Table 1, the cohesion and angle of internal friction values of the subgrade and aggregate layers are not given.
Response: Table 1 reports the typical material properties used in the FE models developed to investigate the stress-deformation response of unpaved road constructed on weak or marginalized soil subgrade and subjected to quasi-static or quasi-dynamic loading scenarios. It is to be noted that Table 1 specifically reports the magnitudes of unit weight and stiffness

parameters that are adopted in the present study. The adopted magnitudes conform to the reasonable range of the corresponding parameters that are encountered in the construction materials of such unbounded roads and reported in relevant literature (Meen *et al*., 2013; Yaghoubi *et al*., 2016). It is also to be noted that the specific strength parameters of the marginalized subgrade (cohesion, c_{sub}, and angle of internal friction, φ_{sub}) are not mentioned in Table 1. In the latter half of the manuscript, Section 5.1 and Section 5.2 utilizes different magnitudes of the strength parameters to elucidate the influence of quasi-static and quasi-dynamic loading scenarios, respectively, on the response of FE model. Thus, the specific magnitudes of the shear strength parameters are explicitly mentioned thereof and, hence, is not mentioned in Table 1 as typical magnitudes. The caption of Table 1 is also slightly modified.

Comment 3: What is the thickness of the subgrade and aggregate layers? How did the authors choose the thickness of the pavement layers? The authors should clarify it in the manuscript.

Response: The current study pertains to the unpaved roads that comprise of an unbounded aggregate layer directly placed over the soil subgrade. The thickness of the aggregate layer is governed by the bearing strength of the subgrade layer and the vehicular load it has to carry. Hence, for the FE simulations, the thickness of the aggregate layer is adopted as per the solution obtained from Equation 3 (in the revised manuscript) based on the specific magnitudes of the contributing parameters. As for the soil subgrade layer, it is considered as a semi-infinite homogeneous medium. The thickness is chosen in such a way that the stresses/strains/deformations developed beneath the aggregate layer is not intersected or influenced the bottommost fixed boundary of the soil subgrade. The clarifying statements in this regard are added in the revised manuscript.

Comment 4: A validated model is not used for further analysis. Then, what is the significance of the validation part of the manuscript?

Response: It is important to conduct a validation study to understand the capability of the developed FE methodology in capturing the stress-deformation response from a chosen constitutive model. Such validation studies are conducted primarily to gain confidence on the developed numerical model such that it can represent the experimental findings to an acceptable extent. In this regard, a suitable experimental investigation is chosen in similitude to the considered problem, and the suitability of the developed FE model and the adopted constitutive relationships is judged based on the similarity in the outcomes from the numerical analysis and experimental investigations. Once the numerical model is validated, the same

model itself can be further used, especially for parametric investigations. However, it is not mandatory to proceed with the validated model for further research. If the suitability of the numerical methodology and constitutive relationships is already established through the validated model, the geometrical dimensioning and the material properties of the validated model can be altered to suit the actual research problem, as long as the relative geometrical configuration and constitutive behaviour of the individual components of the FE model is not altered. In the present study, the FE model of the unpaved road comprises two layers (aggregate layer overlying the subgrade layer) with loading from dual wheel (representing the quasi-static vehicular load) on an equivalent rectangular tire-contact area over the aggregate layer (as shown in Fig. 2 in the revised manuscript). In absence of an exact experimental representation of quasi-static loading on an unpaved road system, for the present study, the validation is carried out with respect to an experimental investigation by Roy and Deb (2019). The stated experimental investigation (Roy and Deb, 2019) deals with the interference effect of two closely-spaced identical footings resting on granular fill of limited thickness over soft clay and, accordingly, a corresponding FE model is developed (as shown in Fig. 4 in the revised manuscript). Both the FE models, i.e. one that used for unpaved roads (Fig. 2 in the revised manuscript) and the one used for validation study (Fig. 4 in the revised manuscript), have the same physical structure of double-layered soil system with a granular layer overlying the marginalized or soft soil layer. For both the models, closely spaced interfering rectangular areas placed over the granular layer subjected to uniformly distributed loads is considered. For both the models, the granular fill and soft clay is represented by the Mohr-Coulomb constitutive relationship. Hence, in light of these similarities, if the FE model for validation study (Fig. 4 in the revised manuscript) shows agreeable results with the experimental investigations, the FE model unpaved road (Fig. 2 in the revised manuscript) can also be considered validated as long as it follows a similar relative geometrical configuration and utilizing the same constitutive relationship for the different components of the numerical model. A note in this regard is added in the revised manuscript.

Comment 5: Section 4.3, Normally, R_{inter} is considered less than 1 for the interface of soil and geosynthetic material. Why did the authors choose a high R_{inter} value in this study?

Response: The strength of the interface is governed by the strength reduction factor (R_{inter}) value, signifying the roughness of interaction between two dissimilar materials while they are shearing to each other. Generally, R_{inter} value ranges between 0 (zero) to 1 (one). A value of R_{inter} = 0 signifies the interface to be smooth and full slippage is allowed, while a value of 1

(one) emulates perfect bonding through a rough interface where no slippage is allowed. In the present study, the interface is provided between two materials i.e. soil subgrade and geotextile and that between geotextile and aggregate. In most geotechnical engineering problems involving shearing of one medium over the other, the magnitude of R_{inter} is maintained less than one as one material is allowed sliding over the other. For example, in slope stability problems involving soil-geosynthetic interfaces, it is a common practice to consider the critical strength at the interfaces, and hence R_{inter} value can range between 0.4-0.7 [64, 65]. However, in the present study, the aggregate-geosynthetic and geosynthetic-subgrade interface is meant to bear the compressive loads and is expected to undergo minimal shearing induced slippage along the length of the geosynthetic. Further, the aggregate-geosynthetic interface is supposed to be quite rough so that slippage is prevented and the membrane action of the geosynthetic is triggered from stretching of the geosynthetic owing to the lateral stresses transferred from the aggregate layer to the geosynthetic interface. As the aggregate and geosynthetic is considered in perfect bonding to each other without any slippage, R_{inter}=1 is assumed in the present study. Although briefly explained in the earlier submission, in the revised manuscript, a description related to the consideration of R_{inter} value is further added along with some amendments in the earlier statements.

Comment 6: Section 4.3.2: Why did the author consider this loading pattern?

Response: A FE-based study is conducted to decipher the effect of vehicular load repetition on the behaviour of unreinforced and reinforced unpaved road. The problem is tackled as a quasi-dynamic problem. In this case, the actual time-dependent spatial movement of the vehicle is represented in terms of the axle load repetitions at specific intervals of time. This is conveniently represented by a triangular or Haversine loading of specific duration (denoting the passage time of the vehicle through the specific section of the road) and repeating at a specific time interval (denoting the passage of successive similar vehicles). In such consideration, the main parameters of load repetition that are considered comprise the equivalent contact stress at the tire-aggregate interface ($P/2BL$), number of load passes (N), time gap between the arrival and departure of the vehicle through a road section (t') and time interval between two consecutive passes (Δt). Following such consideration, the input signal of quasi-dynamic vehicular load is considered to be triangular or Haversine in nature to give a realistic view of the multi-vehicular passage through a common section (Shen and Carpenter, 2007; Tao and Abu-Farsakh, 2008; Abu-Farsakh and Chen, 2011; Vern et al. 2016; Ingle and Bhosale, 2017; Demir et al., 2018; Leonardi et al., 2020). The two arms of the

triangular/Haversine input signify the approach (rising arm of the loading) and departure (falling arm of the loading) of a vehicle through the particular section of the road. In the present problem, as shown in Fig. 8 (in the revised manuscript), the quasi-dynamic load is applied through dynamic load multipliers repeated at regular time interval (Δt) of 2 s. The approach of a vehicle (denoted by the rising arm of the triangular input) takes place over a time span of 0.1 s, following by its departure (denoted by the rising arm of the triangular input) from the same section in the next 0.1 s. Hence, the overall time duration of the passage of vehicle over a particular section (t') is 0.2 s. Figure 9 (in the revised manuscript) depicts a typical displacement profile observed beneath the wheel for a single passage of the vehicle. It can be noticed that during the interval 0.2-0.4 s, the displacement follows the haversine triangular pattern in congruence to the applied triangular load. Furthermore, interestingly, as the vehicle departs, an elastic rebound is observed for around 1.2-1.3 s, beyond which the displacement culminates to a residual magnitude. Hence, in the present study, the next vehicular pass is considered at a time interval after the completion of the elastic rebound, and accordingly a conservative resting time interval of 2 s is adopted before the application of next passage of the similar vehicle. However, any other time interval could have been also considered depending upon the actual traffic passage through the road section. In the present study, identical vehicle passages are considered, and the influence of mixed mode vehicular configuration is kept out of scope from the analyses. Although briefly discussed in previous submission, an elucidated note is provided in the revised manuscript with due modifications and amendments.

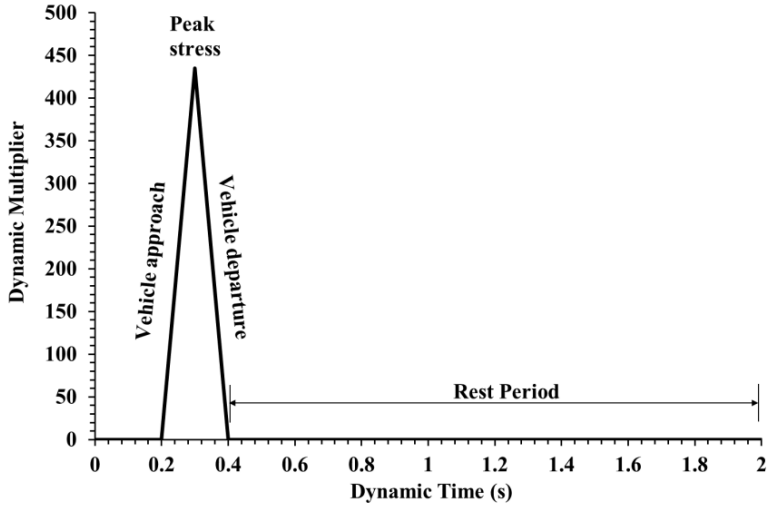

Fig. 8 Triangular load distribution signifying the quasi-dynamic multiplier for single vehicular passage

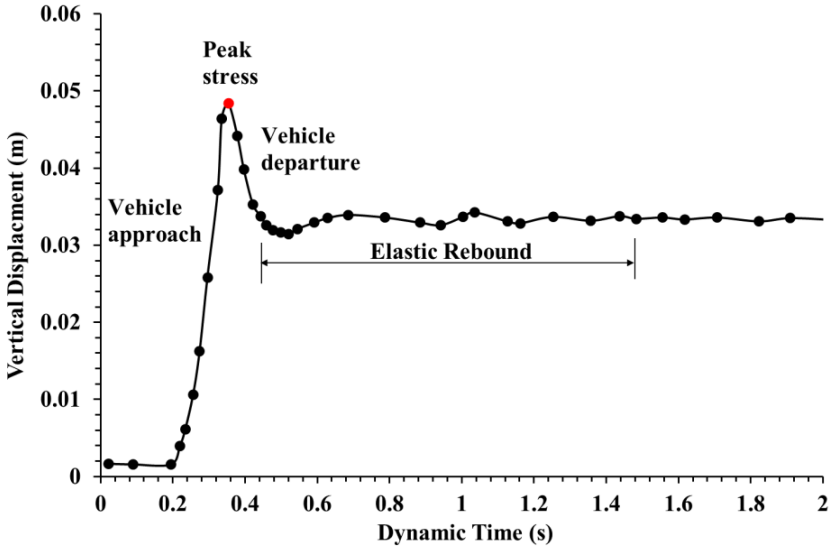

Fig. 9 Variation of vertical displacement beneath the wheel for a single passage of vehicle

Comment 7: Section 5.1.1, line no. 30, figure number is missing.

Response: The missing figure number is now added (Figure 10) in the revised manuscript.

Comment 8: Section 5.2: How was the number of passes for the repetitive vehicular loading determined?

Response: Thank you for the comment. As such, the number of vehicle passes were arbitrarily chosen to begin with the simulations. However, the primary emphasis was given to the vertical displacement generated due to repeated loading and its agreeability to the failure criterion of the unreinforced or reinforced unpaved road. In this case, the failure criterion is governed by the limiting rut depth of 75 mm to be maintained for the serviceability of the unpaved road as given in the standard literatures (Giroud and Noiray, 1981; Holtz and Sivakugan, 1987; ASTM E1703/E1703M-10, 2015; Sarma and Dey, 2024).

Comment 9: Kindly provide the figure of the 3D FE model of reinforced pavement.

Response: In the revised manuscript, a figure of the 3D FE model of reinforced unpaved road is now provided (Fig. 7).

Comment 10: In the Result and Discussion section, please provide some comparisons between your data and other published literature.

Response: Thank you for the valuable comment. In accordance to the suggestion, relevant comparisons and discussions in light of previous published literature has been added at appropriate locations in the 'Results and Discussions' section in the revised manuscript. The

qualitative and quantitative mentions about various findings are provided; namely the strains generated in unreinforced and reinforced unpaved sections (Hufenus *et al*., 2006; Ingle and Bhosale, 2017), magnitudes of rutting for repeated loading (Perkins et al., 2012; Wu et al., 2015; Ingle and Bhosale, 2017) and percentage improvement in surface displacements due to the application of varying geosynthetics of different tensile modulus (Leonardi et al., 2000; Latha et al., 2010; Nair and Latha, 2016; Singh et al., 2022).

Comment 11: Editorial corrections are required throughout the manuscript: it should be Figure 1 instead of Fig. 1 at the start of the new line (Page 5, line 23). Similar corrections need to be made throughout. A few sentence corrections are required (e.g., page 22: lines 26-29; page 23: lines 54-57). Check for it throughout the manuscript.

Response: Thank you for the comment. In the revised manuscript, all the editorial corrections have been taken care of to the best of authors knowledge.

Response to Reviewer-2 Comments

Reviewer #2: I have reviewed the paper "Improvement of Long-Term Performance of Unpaved Road constructed over marginalized Subsoil using Geotextile Reinforcement". Overall, the paper brings an interesting idea for a research topic, even though there are many publications related to the concept not cited in the paper. I strongly recommend the authors to improve the literature review. There are just a few papers cited in the paper of the last four years. It is very important trying to compare the current results to previous investigations. In the results session, the authors must better explain why they obtained the observed behaviors and if they agree to other investigations. There is a conceptual mistake in several figures: deformation is different from displacement. The unit of the first is "%" and for the second is "m" or "mm".

Response: Thank you for the comment. In the revised manuscript necessary changes in the manuscript has been conducted. As per the suggestion of the reviewer, the authors have significantly improved the literature review, with more publications from the recent years being cited and their significance in the research domain being mentioned in the ‘Introduction’ section of the revised manuscript.

Furthermore, in accordance to the valuable suggestion, relevant comparisons and discussions in light of previous published literature has been added at appropriate locations in the ‘Results and Discussions’ section in the revised manuscript. The qualitative and quantitative mentions

about various findings are provided; namely the strains generated in unreinforced and reinforced unpaved sections (Hufenus *et al*., 2006; Ingle and Bhosale, 2017), magnitudes of rutting for repeated loading (Perkins et al., 2012; Wu et al., 2015; Ingle and Bhosale, 2017) and percentage improvement in surface displacements due to the application of varying geosynthetics of different tensile modulus (Leonardi et al., 2000; Latha et al., 2010; Nair and Latha, 2016; Singh et al., 2022).

Thanks you for highlighting the conceptual mistake in the figures related to deformation and displacement. The corrections have been applied to the relevant figures and their associated texts in the revised manuscript.

Comment 1: Authors need to better explain how they calculated an axis load of 360 kN. It is 36 tons. How did you get this value?

Response: Two different vehicular axle loads of high magnitudes, 360 kN and 190 kN, are used in this study for quasi-static and repetitive vehicular loading analyses (Giroud and Noiray, 1981; Milligan et al., 1989b; MORTH, 2000). The high axle loads considered here are common for heavy haul caterpillar dump trucks (https://www.easternplanthire.com/2020/01/10/the-worlds-top-5-biggest-mining-dump-trucks-2020) and are specifically considered for the present study to distinctively elucidate the robustness of the FE-based design algorithm described in the latter sections of the manuscript. In the revised manuscript, necessary references and relevant note is now included.

Comment 2: In Table 1, what are the values of soil friction angle and cohesion?

Response: Table 1 reports the typical material properties used in the FE models developed to investigate the stress-deformation response of unpaved road constructed on weak or marginalized soil subgrade and subjected to quasi-static or quasi-dynamic loading scenarios. It is to be noted that Table 1 specifically reports the magnitudes of unit weight and stiffness parameters that are adopted in the present study. The adopted magnitudes conform to the reasonable range of the corresponding parameters that are encountered in the construction materials of such unbounded roads and reported in relevant literature (Meen *et al*., 2013; Yaghoubi *et al*., 2016). It is also to be noted that the specific strength parameters of the marginalized subgrade (cohesion, c_{sub}, and angle of internal friction, φ_{sub}) are not mentioned in Table 1. In the latter half of the manuscript, Section 5.1 and Section 5.2 utilizes different magnitudes of the strength parameters to elucidate the influence of quasi-static and quasi-

dynamic loading scenarios, respectively, on the response of FE model. Thus, the specific magnitudes of the shear strength parameters are explicitly mentioned thereof and, hence, is not mentioned in Table 1 as typical magnitudes. The caption of Table 1 is also slightly modified.

Comment 3: In the validation study, it was not explained the boundary conditions and if the analysis was conducted in drained or undrained condition? An undrained condition can lead to the local failure of the soft soil layer underneath the tires and this can imply higher displacements.

Response: The experiment by Roy and Deb (2019) was conducted within a steel tank. Hence, as per the experimental set up, in the numerical model, the bottom boundary of the soft clay layer is fully fixed against vertical and horizontal displacements, while, along the lateral boundaries, only horizontal fixities are provided. As per the information from experimental investigations, the soft clay was maintained at an undrained condition, while the presence of sand bed provided a drained condition in the overlying layer; the same is maintained in the numerical model. The loading rate in the numerical model is maintained at 2 mm/min in conformity to the rate of loading in the experimental investigation.

Comment 4: Insert the methodology of the item 4.2 as a table.

Response: The authors checked in the draft revision the visual aesthetics of putting the methodology in a table format. However, none additional benefits are noticed in this way, either in aesthetics or in saving of space in the manuscript. The visual easiness is provided by the supplementing flowchart, which was already present in the original manuscript. Hence, the methodology of Section 4.2 in maintained unchanged in a listed form in the revised manuscript as well.

Comment 5: Item 5.1: A 0.77 m length tire contact as well as the value for the width (0.55 m) are very large values. There are other researches which used lower values. Please, improve the literature about it and better explain why these values.

Response: In the present study, a dual wheel system truck is considered as they are more prevalent than single wheel version on unpaved roads. In a dual wheel system, it is considered that the soil in-between the tires get mechanically associated with the wheels. As it is understood that the mechanically associated soil or aggregate between the tires would not undergo failure, they represent a composite or equivalent contact area that is larger than twice the actual contact area of each tire (Giroud and Noiray, 1981; Meena et al., 2013). Accordingly,

considering on-highway vehicles, the width of the equivalent contact area is given as $B = \sqrt{P/P_c}$ and $L = B/\sqrt{2}$; for off-highway vehicles the same is denoted as $B = \sqrt{P\sqrt{2}/P_c}$ and $L = B/2$ (Giroud and Noiray, 1981). Accordingly, in the present study, based on the chosen magnitudes of P and P_c, the equivalent contact dimensions are estimated as B = 0.77 m and L = 0.55 m. A note on the same is provided in the revised manuscript.

Comment 6: Figure 8 does not bring much as a result. Furthermore, there is not any discussion about it. I suggest you remove it.

Response: The figure has been renumbered as Figure 10 in the revised manuscript. The figure is important in depicting the state of deviatoric strains propagating in the subgrade through the aggregate-subgrade interface, thereby indicating that the subgrade strength (for this case) is not sufficient to bear the aggregate loading itself, thereby necessitating a ground improvement technique. Figure 10 is important to be given for substantiating this observation, and hence, the same is maintained in the revised manuscript as well. In Step 3 of Section 5.1.1, the figure number was inappropriately missing in the previous submission. The same has been included as pointed out by Reviewer 1.

Comment 7: Page 18: In the discussion of the "5.1.1 Outcomes from a typical FE-based simulation for unreinforced unpaved road", there are some issues to be better addressed: is the analysis considered in a drained or undrained condition? What were the drainage conditions at the boundaries and interfaces?

Response: In the numerical analyses, analyses are considered under ‘drained’ condition. The effect of any water table conditions is left out of scope of the present work.

Comment 8: Page 21: I do not understand why to increase the cohesion to 1.88 if the idea is to insert the geotextile element. Would not be easier to calculate a Factor of Safety and if it is less than one the geotextile is recommended?

Response: In case of subgrades with lesser strength than that desired, a common approach to enhance the strength of the subgrade is by adopting some ground improvement techniques. In general, either soil replacement or soil stabilization by admixtures. For long stretches of road, the latter find more practical usage. In this process, mostly the cohesive characteristics of the strength gets enhanced. Thus, in order to show the utility of such ground improvement technique in improving the strength of the subgrade to bear the operational loading conditions,

a minimal increase in the cohesion is highlighted for a particular case as an example (in Section 5.1.1). However, given the fact that the selection of ground improvement techniques depends on several factors such as type of soil, geographical structure, seepage conditions, degree of improvement required, availability of equipment and material, available construction time, durability and reusability of materials used, environmental conditions, and finally the cost of project which might be a decisive one. These factors increase the overall cost of construction and consumption of raw materials for the construction. In this regard, inclusion of geosynthetics as reinforcement provides a more practical and cost-effective solutions to such problem. Thus, for the reinforced unpaved road analysis (as in Section 5.1.2), as an alternative to ground improvement measures by increasing the cohesion, geosynthetics are used as planar reinforcement to enhance the bearing capacity of the system. Hence, in Section 5.1.2, the cohesion is not increased further and the beneficial usage of geosynthetic reinforcement is highlighted. This is in tune with the observation made by the reviewer, and is already described in the manuscript. However, instead of going to assessing the factor of safety (FoS), the authors banked upon the stress-deformation and formation of slip planes to take the confirmative decisions. FoS can also be used, but the authors deliberately avoided going into limit equilibrium techniques that has its own shortcomings by not considering any deformation into the analysis. To make the discussion clarified, relevant portions of this note is included in the revised manuscript.

Comment 9: Figure 13: authors must insert x and y axis. The way the figure is being represented, the rutting is higher than half of the embankment height.

Response: In Figures 15b and 16 (renumbered from Figures 13 and 15 in the original manuscript), the scaling of the rutting deformation are not in conformity to the scaling of the aggregate layer thickness (which is of much higher magnitude). The exaggerated scaling of rutting magnitudes is provided for giving a comparative visualization from different numbers of vehicle passes. Hence, just by providing axes labelling will not help the cause. A note is added in this regard in the corresponding text as well as the caption of Fig. 15 in the revised manuscript.

Comment 10: Why in Figure 14 the maximum vertical displacement is equal to 0.17 m for 10 vehicle passes and in Figure 15 this value is less than 0.10 m for the unreinforced case if the amount of vehicle passes is the same? By the way, are not these values high for only ten vehicle passes? Authors must compare their results to similar publications.

Response: Figure 14 (renumbered as Figure 16 in the revised manuscript) shows the accumulation of vertical displacement at the mid-point of the equivalent rectangular wheel load distribution on the surface of aggregate layer (shown as Point A in Fig. 15a of the revised manuscript as well as in the adjacent figure). However, in Figure 18 (in the revised manuscript), the vertical displacement is depicted averaged over the section B-B (shown in Fig. 15a of the revised manuscript as well as in the adjacent figure) connecting the edges of the wheel load. Hence, both the values are different. The displacement at the center of the wheel is evidently more than that observed in the edges of the wheel, and the same is intended to be shown here. For adding clarity, the locations of the measurement are highlighted with the aid of diagrams in the revised manuscript. Furthermore, in accordance to the valuable suggestion, relevant comparisons and discussions in light of previous published literature has been added at appropriate locations in the 'Results and Discussions' section in the revised manuscript. The values obtained here seems to be satisfactory given that unpaved road undergoes greater rutting in comparison to the paved road systems; magnitudes of similar order are reported in other studies as well, and same has been mentioned at relevant places in the revised manuscript.

Comment 11: Authors must reorganize the conclusions. Some of them are not conclusions based on the manuscript results. For example, the first conclusion is only an abstract about the methodology.

Response: As per the suggestion, the conclusions have been reworked based on manuscript results.